

# **A Study on the Factors causing the Enhanced Inland Penetration of Monsoon Depressions into the Indian Landmass**

**A Thesis**

submitted to

Indian Institute of Science Education and Research Pune in partial fulfilment

of the requirements for the BS-MS Dual Degree Programme

by

**Sandhya Vijayan K**



Indian Institute of Science Education and Research Pune

Dr. Homi Bhabha Road,

Pashan, Pune 411008, INDIA.

April 2023

**Supervisor: Dr. Sooraj K.P, IITM, Pune**

**Expert: Dr. Suhas Ettamal, IISER, Pune**

© Sandhya Vijayan K 2023

All rights reserved

*Dedicated to my Achan, Amma and Ettan*

# Certificate

This is to certify that this dissertation entitled '**A Study on the Factors causing the Enhanced Inland Penetration of Monsoon Depressions into the Indian Landmass**' towards the partial fulfilment of the BS-MS dual degree programme at the Indian Institute of Science Education and Research, Pune represents study/work carried out by Ms. Sandhya Vijayan K at Indian Institute of Tropical Meteorology under the supervision of Dr.Sooraj K P, Scientist E, Center for Climate Change Research, during the academic year 2022-2023.



Dr.Sooraj K P

Scientist E

Center for Climate Change Research

Indian Institute of Tropical Meteorology, Pune

Committee:

Dr. Sooraj K P

Dr. Suhas Ettamal

# Declaration

I hereby declare that the matter embodied in the report entitled '**A Study on the Factors causing the Enhanced Inland Penetration of Monsoon Depressions into the Indian Landmass**' are the results of the work carried out by me at the Center for Climate Change Research, Indian Institute of Tropical Meteorology, Pune, under the supervision of Dr. Sooraj K P and the same has not been submitted elsewhere for any other degree.



Sandhya Vijayan K

20181196

BSMS

IISER Pune

# Acknowledgments

I am highly indebted to my supervisor, Dr. Sooraj K P for providing me with an opportunity to work on the project under his guidance. His valuable time, constant support and suggestions were instrumental in the effective execution of this project. I also owe a great deal of gratitude to my thesis expert, Dr. Suhas Ettamal, for motivating me to conduct the project and providing helpful feedback on our work. I acknowledge the director of the Indian Institute of Tropical Meteorology, the director of the Centre for Climate Change Research, and other supporting personnel for providing the necessary facilities in IITM, without which I would not have been able to perform efficiently on this project. I also appreciate IISER Pune for giving me the chance to work on a research issue. I express my heartfelt thanks and affection to my family and friends for their unconditional support.

# Contents

|   |           |
|---|-----------|
| <b>List of figures</b> .....  | <b>7</b>  |
| <b>List of tables</b> .....   | <b>10</b> |
| <b>List of abbreviations</b> .....  | <b>11</b> |
| <b>Abstract</b> .....   | <b>12</b> |
| <b>1. Introduction</b> .....  | <b>13</b> |
| 1.1 Monsoon depressions (MD).....   | 14        |
| 1.1.1 Structure.....  | 15        |
| 1.1.2 Propagation mechanism.....  | 16        |
| 1.2 Inland penetration of MD.....   | 18        |
| 1.2.1 Soil moisture- MD relation.....   | 19        |
| 1.2.2 Mid-tropospheric cyclone (MTC) - MD relation.....   | 21        |
| <b>2. Data and Methodology</b> .....  | <b>23</b> |
| <b>3. Results and Discussion</b> .....  | <b>28</b> |
| 3.1 Mean statistics on frequency and duration of MDs.....   | 28        |
| 3.2 Spatio-temporal analysis of anomalous precipitation and selection of<br>long-lived and short-lived MDs..... | 31        |
| 3.3 Soil moisture analysis.....   | 35        |
| 3.4 Relation of MTC to long-lived and short-lived MDs.....  | 37        |
| <b>4. Summary and conclusions</b> .....   | <b>53</b> |
| <b>References</b> .....   | <b>56</b> |

# List of figures

|   |    |
|---|----|
| <b>Figure 1.</b> A schematic diagram showing rectangular boundary of the chosen central Indian region for identification of extreme rainfall events.....  | 24 |
| <b>Figure 2.</b> Tracks of MDs for (a) June, (b) July, (c) August, and (d) September.....   | 28 |
| <b>Figure 3.</b> Lifetime statistics of MDs during the boreal summer monsoon season of 1991-2020 (30 years).....  | 30 |
| <b>Figure 4.</b> A bar diagram showing how far the MDs can travel over land after hitting the coastline and the number of MDs for each range of inland penetration lengths for the period 1991-2020.....  | 30 |
| <b>Figure 5.</b> (a) Composite plot for precipitation anomaly for depression days (b) Composite plot for depression days which caused extreme rainfall events over central India bounded by the coordinates 20-25°N latitudes and 73-81°E longitudes..... | 31 |
| <b>Figure 6.</b> The daily evolution of anomalous precipitation for 21 MD events that caused extreme rainfall over central India (20 - 25°N and 73-81°E).....   | 32 |
| <b>Figure 7.</b> The relative longitude-latitude plot of contrast between the TOP and BOTTOM soil moisture content above the Day 2 region from Day 2 to Day -1. The coordinate origin is centered with respect to relative vorticity maxima.....          | 35 |
| <b>Figure 8.</b> A composite of the daily evolution of precipitation anomaly for (a) TOP (left panel) and (b) BOTTOM (right panel) cases.....   | 38 |
| <b>Figure 9.</b> Tracks of MDs with 850 hPa relative vorticity anomaly maxima as the storm center for (a) TOP cases (b) BOTTOM cases.....   | 39 |
| <b>Figure 10.</b> Composites of the horizontal pattern of relative vorticity anomaly at 500 hPa pressure level from Day -5 to Day 3 (Day 0 being the landfall day) for TOP cases.....   | 40 |

**Figure 11.** Composites of the horizontal pattern of relative vorticity anomaly at 850 hPa pressure level from Day -5 to Day 3 for TOP cases.....41

**Figure 12.** Composite of the evolution of vertical integral of divergence of moisture flux ( $\text{kgm}^{-2}$ ) over Indian region from Day -3 to Day 2 for TOP cases.....42

**Figure 13.** Horizontal pattern of relative vorticity anomaly (shaded) and wind velocity anomaly (vectors) from Day -3 to 2 (2007-08-06 - landfall day) for an MD during 2007 Aug 5-8 (an example from the TOP list) at (a) 500 hPa, and (b) 850 hPa.....43

**Figure 14.** Horizontal pattern of VIDMF anomaly from Day -3 to 2 (2007-08-06 - landfall day) for MD during 2007 Aug 5-8 (an example from TOP list).....44

**Figure 15.** Storm centered horizontal composite plots of relative vorticity anomaly at 850 hPa for TOP case. Regions are categorized according to when and where they fall within a specific longitudinal range.....44

**Figure 16.** Storm-centered vertical composite plots of relative vorticity anomaly at different pressure levels for the TOP case. (a) latitudinal cross-section (b) longitudinal cross-section.....45

**Figure 17.** Composites of the horizontal pattern of relative vorticity anomaly at 500 hPa pressure level from Day -5 to Day 3 (Day 0- landfall day) for BOTTOM cases.....46

**Figure 18.** Composites of the horizontal pattern of relative vorticity anomaly at 850 hPa pressure level from Day -5 to Day 3 for BOTTOM cases.....47

**Figure 19.** Composite of the evolution of vertical integral of divergence of moisture flux ( $\text{kgm}^{-2}$ ) over Indian region from Day -3 to Day 2 for BOTTOM cases.....47

**Figure 20.** Horizontal pattern of relative vorticity anomaly (shaded) and wind velocity anomaly (vectors) from Day -3 to 2 (2011-09-22 - landfall day) for an MD during 2011 Sept 22-23 (an example from the BOTTOM list) at (a) 500 hPa, and (b) 850 hPa.....49



**Figure 21.** Horizontal pattern of VIDMF anomaly from Day -3 to 2 (2011-09-22 - landfall day) for an MD during 2011 Sept 22-23 (an example from the BOTTOM list).....50

**Figure 22.** Difference between VIDMF ( $\text{kgm}^{-2}$ ) of composite TOP and composite BOTTOM.....50

**Figure 23.** Hovmöller diagram of relative vorticity anomaly from Day -5 to Day 5, with longitude on the x-axis (a) at 850 hPa and(b) at 500 hPa. Values are latitudinally averaged between 15-26°N. Upper panel figures show TOP composites and lower panel figures show BOTTOM composites.....51

**Figure 24.** Hovmöller diagram of VIDMF from Day -5 to 5, with longitude on the x-axis (latitudinally averaged between 15-26°N). Left side- TOP composite, and right side- BOTTOM composite.....52

# List of tables

**Table 1.** Month Wise statistics of MDs for the period 1991-2020.....29

**Table 2.** List of the TOP 10 MDs, their inland penetration lengths (IPL), and the dates of Northeastern Arabian Sea MTC, if any occurred during the lifetime of MD.....33

**Table 3.** List of BOTTOM 10, their inland penetration lengths (IPL), and the dates of Northeastern Arabian Sea MTC, if any occurred during the lifetime of MD.....34

# List of abbreviations

|       |  |
|-------|--|
| BoB   | Bay of Bengal                                      |
| CISK  | Convective Instability of Second Kind              |
| ECMWF | European Center for Medium-Range Weather Forecasts |
| EPV   | Ertel's Potential Vorticity                        |
| ERA-5 | ECMWF Re-Analysis version 5                        |
| GLDAS | Global Land Data Assimilation System               |
| IMD   | Indian Meteorological Department                   |
| IPL   | Inland Penetration Length                          |
| ISMR  | Indian Summer Monsoon Rainfall                     |
| ITCZ  | Intertropical Convergence Zone                     |
| JJAS  | June, July, August, September                      |
| LPS   | Low-Pressure Systems                               |
| MD    | Monsoon Depressions                                |
| MTC   | Mid-Tropospheric Cyclone                           |
| NOAA  | National Oceanic and Atmospheric Administration    |
| PV    | Potential Vorticity                                |
| QGPV  | Quasi-Geostrophic Potential Vorticity              |
| VIDMF | Vertical Integral of Divergence of Moisture Flux   |
| WRF   | Weather Research Forecast                          |

# Abstract

Monsoon Depressions (MDs) are low-pressure systems that form over the Bay of Bengal (BoB) during boreal summer, thus constituting more than half of the ISMR. The inland penetration and duration of MDs over Indian landmass are significant as they can regulate the spatiotemporal variability of ISMR. We utilized GLDAS reanalysis data for soil moisture to understand its role in the persistence of landfalling MDs, by a comprehensive examination of the long-lived (TOP 10 cases) and short-lived MDs (BOTTOM 10 cases). This is the first qualitative application of the soil moisture data for ascertaining the relationship of soil moisture with the long residence time of MDs over Indian landmass. Our result reveals that long-lived MDs had higher soil wetness over the area ahead of the MD, compared to short-lived MDs. We also analyzed different dynamical and thermodynamical meteorological parameters using ERA-5 reanalysis data. Interestingly, all 10 TOP cases had preceding cyclonic circulation at mid-troposphere over the northeastern Arabian Sea (i.e., Mid Tropospheric cyclones, MTCs), whereas only 1 MD is accompanied by MTC in the BOTTOM group. In BOTTOM cases, dry air intrusion from heat-low regions creates background moisture conditions unfavorable for the sustenance of the MD structure. The cyclonic vorticity associated with MTC transports moist Arabian sea air to the Indian subcontinent and thus explains the observed increase in convergence of vertically integrated moisture flux over northwest India for TOP cases. Overall, our results provide the first seminal evidence that the presence of MTC over the northeastern Arabian sea, which in conjunction with wet soil conditions create favorable moisture and circulation conditions for a prolonged duration as well as deeper penetration of MD over the Indian subcontinent.

# 1.Introduction

The Asian monsoon system with unique seasonal patterns of precipitation and circulation is a self-regulating large-scale ocean-atmosphere coupled phenomenon that plays a significant role in the weather and hydrological cycle of the planet by transporting oceanic moisture content to the largest continent in the world (e.g., Webster et al., 2002). The Indian summer monsoon, which starts in June and lasts through September (JJAS), is an indispensable part of the Asian summer monsoon and has a profound impact on the lives and economic fortunes of the inhabitants of the Indian subcontinent. Intertropical Convergence Zone (ITCZ), which is the low-pressure belt usually located near the equator where the trade winds from both hemispheres converge, migrates northward to the Indian subcontinent during JJAS (Gadgil, 2018). Due to the Coriolis effect, Southeasterly trade winds south of the ITCZ change their direction when they cross the equator and become southwesterly. So, the Boreal Summer season is also known as the 'Southwest monsoon'.

The southwest monsoon is embedded with synoptic-scale (2-10 days) cyclonic disturbances of a wide range of intensity, collectively termed 'Low Pressure Systems' (LPS; Mooley, 1973; Sikka, 1977; Krishnamurthy and AjayaMohan, 2010). The Indian Meteorological Department (IMD) classified LPS into lows, depressions, deep depressions, and cyclones based on their peak wind speed in cyclonic circulation and pressure anomaly. In the surface pressure chart, a low has one closed isobar with an interval of 2 hPa within the 3° radius of the system's center and has a surface wind speed of less than 17 knots ( $1 \text{ knot}=0.51 \text{ ms}^{-1}$ ). Depressions and deep depressions have wind speeds in the range of 17 -27 knots and 28-33 knots, respectively, with two or three closed isobars in a 3° radius from the center. Cyclones are stronger systems having 34 knots or more of surface wind speeds and more than 4 closed isobars at 2 hPa intervals within 3° radius. Large vertical wind shear created by strong westerlies at the lower troposphere (Low-level jet) and tropical easterly jet in the upper troposphere inhibits the development of cyclones during JJAS. Additionally, since the disturbances originate adjacent to the coast during monsoon season and spend less time on the ocean, they seldom reach cyclonic storm intensity (Mulky and Banerjee, 1960).

## 1.1 Monsoon depressions (MD)

For the sake of simplicity and comparison with other works, we will refer to systems that have intensity greater than or equal to that of depressions as Monsoon Depressions (MDs), as previous authors have done (Cohen and Boos, 2014; Hunt et al., 2016). They are the dominant systems that drench the Indian subcontinent with heavy precipitation along and near their tracks, accounting for nearly half of the Indian Summer Monsoon Rainfall (ISMR) (Yoon and Chen, 2005). Therefore, the frequency of formation, intensity, track, time spent over land, distance traveled after crossing the coastline, and duration of these efficient rain-bearing systems are crucial in regulating the spatiotemporal variability of ISMR (Sikka, 1977). In particular, the extent of penetration of monsoon depression over the Indian landmass and their subsequent residence time over the landmass are significant as they can cause catastrophic flood conditions with enormous impacts, such as loss of life, disease, etc. Therefore, they have a significant impact on the agriculture and economy of the country.

MDs typically generate either fresh in the humid and warm air over the BoB (*in-situ* -68%) or redevelop over BoB by the intensification of the westward traveling residual lows of the South China Sea (Downstream amplification-32%) and propagate west-northwestward towards the Indian subcontinent (Godbole, 1977; Sikka, 1977, 2006; Saha et al., 1981; Meera et al., 2019). This westward propagation feature of MD is noteworthy since it is against the prevailing low-level monsoon westerly wind flow. Sometimes MDs also form over the land points in central India and the Arabian Sea and move to Indian landmass or move away from it (Krishnamurthy and AjayaMohan, 2010).

The actual genesis mechanism of MDs is relatively poorly understood (Cohen and Boos, 2016), although the roles played by barotropic instability, baroclinic instability, and convective instability of second kind (CISK; Charney and Eliassen, 1964) have been examined in various studies (Mooley and Shukla 1978). No single mechanism proposed so far can account for every observed characteristic, but several mechanisms might cooperate to support the growth and maintenance of MDs. The large-scale conditions that favor the MD genesis include upper-tropospheric easterly waves, residual LPS from the

South China Sea region migrating westward, and slow descending of cyclonic circulations in the mid-troposphere (Sikka, 2006). In addition, the following climatological conditions are suitable for the formation and intensification of MDs: warm sea surface temperatures, low-level cyclonic vorticity, strong vertical wind shear, and abundant moisture content up to mid-troposphere (Sikka, 1977; Ananthkrishnan et al., 1965).

### **1.1.1 Structure**

Observational studies using composited mean structures have shown that MDs have a mean time scale of 2 to 5 days, a horizontal wavelength of 1000 to 2000 km, and a vertical extent of 10 to 11 km (Krishnamurti et al., 1975; Godbole, 1977). The lower troposphere (850 hPa) is where cyclonic vorticity and convergence in MDs are at their highest and it remains cyclonic up to 250 hPa (Sikka, 1978). Anticyclonic vorticity and divergence dominate the circulation at the upper levels (Mulky and Banerjee, 1960). It has been known for some time that the convective ascending motion associated with MD is to the west of the center and the system has a southwest tilt with height. Many earlier authors, like Godbole (1977) and Yoon and Chen (2005) concur that the surface rainfall maximum associated with MD occurs in the west/southwest of low-level vorticity maxima. Mooley (1973) concluded that an assortment of factors including the collocated lower tropospheric convergence maximum, the southwest inclination of the core with height, and cyclonic mixing of warm-moist Indian ocean Southwesterlies and cold easterly from the north are responsible for this shift in location. In a recent work, Hunt et al. (2016b) attributed it to collocated deep convection. Both stratiform clouds and deep convective clouds are responsible for rain that falls associated with MDs (Rao, 1976).

Hunt et al. (2016a) thoroughly investigated the horizontal and vertical structure of BoB MDs as situated over ocean and land, and how it varies in response to various large-scale background states such as El Nino Southern Oscillation, Indian Ocean Dipole, active-break cycle etc. They showed that many dynamic and thermodynamic fields including relative humidity and cloud cover have their peak values in the relative southwest sector in the horizontal cross-section at 850 hPa. Potential vorticity (PV) has a bimodal vertical structure at the center with primary maxima at 500 hPa and secondary maxima at

around 850 to 700 hPa. They also confirmed that almost all MDs have a warm core aloft and cold core nature (Sikka 1978) at low levels with a temperature minimum at relative southwest (Joseph and Chakraborty, 1980; Hunt et al., 2016a). The warm core above is linked to intense latent heat release due to the convective precipitation, and the cold core below is related to decreased insolation as a result of increased cloud cover (Hunt et al., 2016a).

### **1.1.2 Propagation mechanism**

For a long time, Meteorologists have been engrossed by the question of how MDs propagate westward. One of the earliest explanations suggests that the westward movement of MD may be through a feedback mechanism in response to the rainfall maximum occurring in the west (Goswami, 1987). The stationary atmosphere responds to an isolated heat source (the warming of the troposphere resulting from latent heat release related to organized cumulus convective activity due to initial instability is the heat source in this situation) at a latitude around 20°N as a stationary Rossby-gravity wave to the west of the heat source (Gill, 1980) which generates a cyclonic vorticity peak in the northwest zone of the MD. Goswami (1987) demonstrated that maximum moisture convergence and heat source shift to the northwest zone at a later time and the feedback process leads to the movement of MDs in the northwest direction. However, the proposed dynamical model predicted the highest precipitation in the northwest zone which is contradictory to the observed precipitation peak in the southwest zone. Also, the model assumes a constant basic flow, but in reality, it is spatially varying with westerly in the trough's south, easterly in the trough's north, and nearly zero in the trough.

According to Saha and Saha (1988), MD has a strong convergence and divergence to the east and west, respectively in the lower troposphere. Through heat budget analysis of 143 MDs, Yoon and Chen (2005) showed that this asymmetric circulation is maintained by east-west differential diabatic heating. The latent heat release from precipitation over the west sector of MD is mainly responsible (~80%) for the diabatic heating of MD (Saha and Saha, 1988). Water vapor budget analysis showed that MD's rainfall is largely



contributed by the convergence of water vapor flux (Yoon and Chen, 2005). By comparing the equation for the potential of water vapor flux and the velocity potential maintenance equation, it was inferred that east-west divergent circulation is maintained by the release of latent heat from condensation. Based on these characteristics, Chen and Yoon (2005) proposed a mechanism for the westward propagation of MDs. Using stream function budget analysis, they showed that negative stream function tendency is created over the west of an MD center through vortex stretching by the ascending branch (west) of MD's asymmetric divergent circulation, which is thought to be responsible for their westward propagation. Until the supply of water vapor ceases, the whole feedback process will continue to occur.

All the above studies are based on quasi-geostrophic lifting west of the MD center, causing vortex stretching and leading the vortex to shift to the west. Boos et al (2015) confirmed that quasi-geostrophic lifting can provide a qualitative explanation for the horizontal distribution of vertical motion with an ascent over the southwest. However, quantitative analysis of the exact vorticity budget showed that horizontal advection due to the mean flow cancels the vortex stretching. So, the vortex stretching cannot explain the observed westward propagation, rather its purpose is to keep the vortex structure upright which would otherwise be tilted due to horizontal advection by vertical wind shear.

Quasi-geostrophic models have been used by most of the previous studies to comprehend depression dynamics. But, the Rossby number should be less than unity to use quasi-geostrophic approximation, and MDs do not satisfy this condition. If quasi-geostrophic potential vorticity (QGPV) and Ertel's potential vorticity (EPV) fields are similar for a disturbance, dynamics can be still explained by quasi-geostrophic approximation, even if Rossby number is greater than unity (Davis, 1992). However, the QGPV structure has a peak magnitude at low-level and it decays with height whereas EPV has a bimodal distribution with a primary maximum in the middle troposphere and a secondary maximum in the lower troposphere. The complete dynamics of MDs can therefore not really be explained by quasi-geostrophic approximation (Boos et al., 2015).

Considering the importance of the near 500 hPa EPV peak (due to the enhanced static stability of mid-level compared to low-level) that is located above the westerly

background flow, Boos et al. (2015) proposed an alternate theory that MDs propagate north-westward by nonlinear horizontal advection of potential vorticity. They showed that the 500 hPa PV maximum is located in a region with a total wind that is northwest-directed and its magnitude is comparable to the actual MD propagation speed but with a larger component in the north direction. They conducted a PV budget analysis for a case study and the budget equation contains PV tendency due to horizontal advection, diabatic heating, and vertical advection. They suggested that diabatic heating and vertical advection combine to produce PV tendency to the southwest of the storm center and the superposition of this with the PV tendency produced at the north-northwest sector due to adiabatic horizontal advection explains the observed storm propagation. At mid to upper levels, the adiabatic horizontal advection largely contributes to the PV tendency whereas, in lower levels, vertical advective and diabatic tendencies also become important in determining the PV tendency along with horizontal advective tendency.

## **1.2 Inland penetration of MD**

As surface moisture flux and energy flux reduce over land compared to the ocean, the landfalling depressions usually decay quickly. The increase in surface roughness over land will also reduce the wind speeds (Kaplan and DeMaria, 1995) thereby a decrease in relative vorticity and intensity of MD. However, there are cases of lows and depressions that last longer and can penetrate several hundreds of kilometers into the land. They can even re-intensity over land on occasion (Kellner et al., 2012).

It is still not clearly understood whether any large-scale modes of variability influence the duration and dissipation of MDs. Regarding the effect of interannual variability of the ISMR on MD's duration, Krishnamurthy and AjayaMohan (2010) found some evidence for the increased spatial extent of LPS tracks during flood years (reach up to northwest India) compared to drought years (restricted to central India). Krishnamurthy and Shukla (2007) constructed 70-year composites of locations of MDs on depression days (days on which MD is observed in the Indian region) for all active and break periods (intraseasonal modes of Indian Summer Monsoon) during JJAS and found that active

composite has 679 depression days, whereas break composite contains only 105 depression days, indicating that the majority of depression days are connected to active periods. Moreover, since a single MD is represented by multiple depression days equal to its lifetime and since locations are spread across entire central India even up to the northwest region during the active period, more depression days also may be an indication of extended duration and westward propagation of MDs occurring when the monsoon is active. But uncertainty exists regarding the relationship between intraseasonal modes and MDs, that is whether variation in MD formation is caused by differences in large-scale circulations during active and break spells or the spells are caused by variation in the formation of MDs. Also, these studies do not provide a theoretical explanation of how flood years or active spells create atmospheric or land surface conditions favorable for an extended lifetime and deeper inland penetration of MDs. Nevertheless, recent work (Hunt et al., 2016a) has confirmed that MDs strengthen under active monsoon conditions by showing that active spell MDs have lower central pressure, more specific humidity, and amplified warm-over-cold core structure compared to neutral or break spell MDs. They correlated it with an observed increase in 850 hPa cyclonic vorticity (a favorable condition for increased MD activity) over central India on an active-minus-neutral depression days composite plot.

### **1.2.1 Soil moisture - MD relation**

Even Though MDs are synoptic-scale systems and large-scale forcings will prevail in determining their evolution, there are modeling case studies suggesting differences in post-landfall MD activity as the storm made landfall over moist land surface compared with the drier surface (Dastoor and Krishnamurthy, 1991; Emanuel et al., 2008; Chang et al., 2009). Chang et al (2009) conducted numerical experiments on the Weather Research Forecast (WRF) model to explore the possible relation between pre-storm soil moisture conditions over the Indian monsoon region and post-landfall MD structure for three MDs in 2006. The model results show a decrease in surface pressure and an increase in MD precipitation for higher antecedent soil moisture. They also showed that rainfall from the

storm itself only contributes very little to the lowering of surface pressure (~0.5 mb) and the significant contribution (2-3 mb) is from the pre-storm soil moisture.

An observational study of landfalling MDs was conducted by Kishtawal et al. (2013) to test whether the positive relation between antecedent soil moisture and the intensity of storms suggested by the modeling studies can be seen in MD climatology. Because soil moisture data were not available over the Indian region for their analysis period, pre-storm precipitation (7-day average rainfall before the storm genesis) was used as a proxy for ground wetness conditions. They found that MDs with wet pre-storm inland conditions have larger inland penetration length (IPL, how far the storm traveled after crossing the coastline before getting dissipated) compared to dry state MDs, indicating that antecedent ground wetness and landfalling MD activity are strongly coupled. However, this study has limitations as it gives importance only to the soil moisture originated locally and not remotely.

Recently, using a WRF model, Baisya et al. (2017) carried out sensitivity experiments for a case study from October 2013 to understand land-surface precipitation feedback processes and suggest that antecedent soil moisture is key in influencing the precipitation distribution and intensity of an MD. Hunt and Turner (2017) developed numerical experiments using Met Office Unified Model to investigate the nature of the relationship between antecedent soil moisture and MD activity by simulating tracks and structure of a selected MD from August 2014 for varying soil moisture over monsoon trough region and sub-Himalayan arable zone. The resulting tracks suggest that perturbations in soil moisture, both local as well as far away, have the potential to substantially affect the path of a passing MD. The trough zone experiment led to a conclusion that wetter soil conditions cause the strengthening of MD with a stronger bimodal PV structure, warmer mid-tropospheric thermal core, increased axial tilt towards the west, and a longer inland path, and these effects were greatest when the MD was at its most intense stage. However, it is difficult to generalize their results because the simulations were only run for a single MD and so further events need to be looked at using other numerical models.

In a nutshell, to the best of our knowledge, all previous works on soil moisture - MD relation were modeling studies, except Kishtawal et al. (2013) who conducted observational study using antecedent rainfall data. In the backdrop of this, the current study aims to explore the importance of soil moisture (using reanalysis data) on the persistence and intensification of inland penetrating MDs, by a comprehensive examination of the long-lived and short-lived MDs. So this is the first qualitative application of the observed soil moisture data for seeking the relation between the duration of MD and soil moisture.

### **1.2.2 Mid-tropospheric cyclone (MTC) - MD relation**

Mid-tropospheric cyclones (MTC) are quasi-stationary cyclonic systems formed during JJAS over the Northeastern Arabian Sea near the Gujarat state and sporadically over Southern India-China. They are wet synoptic scale disturbances with prominent mid-tropospheric (700-500 hPa) vorticity maxima and weak signatures in the lower troposphere (Carr, 1977; Francis and Gadgil, 2006; Choudhury et al., 2018; Kushwaha et al., 2021). Their vertical thermodynamic structure is somewhat similar to MDs, with a lower tropospheric cold core and a large-scale warm anomaly over 500 hPa (Carr, 1977; Choudhury et al., 2018; Kushwaha et al., 2021). MTCs of the Northeastern Arabian Sea have a crucial role in triggering torrential rains along the west coast of India near Gujarat, which result in significant flooding and devastation in the area (Shyamala and Bhadram, 2006; Kumar et al., 2008; Ray et al., 2019). As a result of the interaction of different dynamic and thermodynamic processes, the development, intensification, and dissipation of mid-tropospheric cyclones remain unresolved. A few factors are the cyclonic vorticity that the continental heat low exports, the wet south-westerly monsoon flow, the orography, the baroclinic instability, the release of latent heat of cumulus convection, and the upper-level easterlies (Ramage, 1966; Mak, 1975; Krishnamurti and Hawkins, 1970; Carr, 1977).

There is observational evidence for the co-occurrence of MTC over the Arabian sea and LPSs over BoB. According to past studies, while LPSs from the BoB are moving westward, MTCs over the Arabian Sea can become more intense (Miller and

Keshavamurthy 1968; Carr, 1977). The main objective of the thesis is to investigate the association of Arabian sea MTC and inland penetration of BoB MD and provide insights into the large-scale environmental conditions and mechanisms conducive for the maintenance or intensification of landfalling MDs. To sum up, while much is known about the structure and intensification aspects of MDs forming over BoB, less is known about the inland penetration of BoB MDs thus warranting detailed studies in this regard. So, keeping this in mind we kept our objectives as following:

1. Does soil moisture conditions over the region ahead of the MD have any influence on its duration and inland penetration length?
2. Is the Arabian sea MTC playing a role in the intensification of MD and its extent of propagation over the Indian landmass?

## 2. Data and methodology

In this study, MDs are identified using weather reports (MAUSAM: Quarterly Journal of Meteorology, Hydrology, and Geophysics: <https://metnet.imd.gov.in/imdmausam/>) as prepared by the Indian Meteorological Department (IMD). MAUSAM online journal published in July each year contains an article on cyclonic storms and depressions formed over the North Indian Ocean one year back, thus providing detailed information regarding the dates, locations, and duration of MDs. IMD reports also contain Arabian sea cyclonic storms, and rarely some BoB depressions that initially propagate in the northwest direction, then recurve and move northeastward moving away from the Indian subcontinent, but we are not interested in those cases. For this study, we have only focused on MDs that originated over the Bay of Bengal, which crossed the eastern coastline of the Indian subcontinent and moved in a west-northwestward direction to the Indian landmass and land depressions that formed close to the east coast of India and moved northwestward during June to September of 1991-2020 (30 years). This identification procedure yielded 70 cases of MD occurrences, including 56 Bay of Bengal depressions and 14 land depressions.

Initially, mean statistics on frequency, duration, and inland penetration length of MDs were determined. In addition to a figure containing tracks of all depressions formed during JJAS of each year, in most cases, especially in recent years, Mausam journal provides the latitude-longitude details of the position of MD as the system evolves. Tracks of only those MDs for which coordinate details are available were reproduced and the behavior of tracks for each month of the summer monsoon season was analyzed. We were unable to plot tracks of MDs for which location coordinates are not provided in the IMD reports, this limits the number of cases we are considering for month-wise track analysis. Statistics on frequency (for each month) and lifetime was determined including all 70 cases and observations are compared with previous studies on MD statistics (eg: Sikka, 1977; Krishnamurthy and Ajayamohan, 2010). The distance (in kilometers) traveled by each MD after landfall was estimated using the lat/long distance calculator on the NOAA website (<https://www.nhc.noaa.gov/gccalc.shtml>) and also using Google Maps

(since there are cases that do not have lat/long information but have information on the place name over which the MD was located). It should be noted that this method is not perfect, so the measurements can only be considered as approximate values for the distance as penetrated by MDs after landfall.

Secondly, the spatiotemporal analysis of anomalous precipitation for the MDs is conducted. For that, we used IMD rainfall data (Pai et al., 2014), which provides high spatial resolution (0.25 x 0.25 degree) 24-h accumulated gridded rainfall data for India. This data is considered to be of high quality and fair representation of the monsoon region's rainfall (e.g., Pai et al., 2015; Choudhury et al., 2018). Precipitation anomaly is calculated by subtracting daily climatology (30-year mean value for each day) from the observed data. Anomalies are used instead of absolute values because they will describe the climatic variability over a region more accurately than absolute values and it is easier to say whether the variable has increased or decreased from normal value for a particular location. Anomaly calculations also allow for meaningful comparisons of different regions. A composite plot of precipitation anomaly for all depression days (a total of 247 days for all 70 MDs) was created to understand how MDs affect rainfall in different regions of India. We identified the daily extreme rainfall events over central India bounded by latitudes 20–25°N and longitudes 73–81°E (Figure 1, the reason for selecting the region is discussed in section 2- Results and discussion).

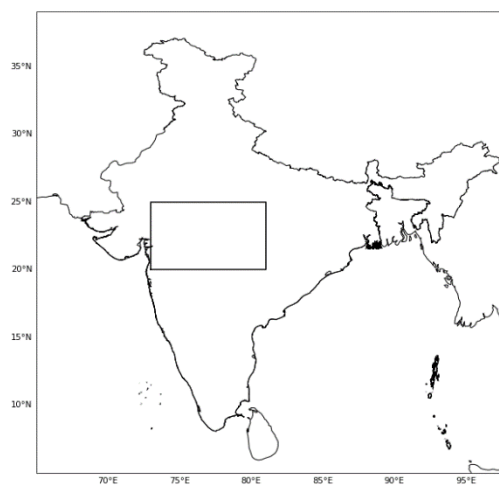


*Figure 1. A schematic diagram showing rectangular boundary of the chosen central Indian region for identification of extreme rainfall events*



The criterion used to identify an extraordinary rainfall event is greater than 150mm in at least 5 grid locations within the chosen region. As heavy precipitation occurs in the vicinity of the MD propagation path, the depression days satisfying the above-mentioned criteria are most likely due to the intense rain-bearing MDs that followed the mean west-northwestward LPS track over central India and intruded farther into the land.

Next, a thorough examination of the MDs that brought extreme rainfall to the chosen region was conducted. For that, precipitation anomaly patterns for each day of the systems are individually examined along with their tracks. The day of landfall and days on which extreme rainfall is experienced over the region of our interest (20-25°N 73-81°E) are noted. Land depressions (we consider only BoB MDs) and the MD cases in which extreme rainfall was experienced during early phases of the system (when the depression was over BoB) were identified and removed. In more detail, an extreme rainfall over central India is assumed to be due to an MD only if the system has already made landfall and moved a significant distance over land. So, if the identified extreme events have occurred when the MD was over BoB and not after intruding into the landmass, such cases are simply avoided. The remaining events are taken into account for analyzing composites of the daily evolution of anomalous precipitation. While creating composite plots of multiple events, a convention is used throughout the work that Day 0 corresponds to the landfall day of each MD event. Accordingly, days prior to landfall and post-landfall are designated by negative (e.g.: Day -1, -2), and positive values (Day 1, Day 2, etc.), respectively.

Among the selected events, 10 MDs that traveled large distances over the Indian landmass are characterized as TOP cases. Among all the 56 BoB depressions, 10 systems that traveled the shortest distances over land are classified as BOTTOM cases.

For the purpose of dynamically tracking the movement of depressions, relative vorticity from the European Center for Medium-Range Weather Forecasts (ECMWF) Re-Analysis version 5 (ERA5, Hersbach et al., 2020) is used. Our study uses daily data with a horizontal resolution of 0.25° x 0.25° (1991-2020). We first calculated the daily climatology of relative vorticity for each day of the JJAS period and subtracted it from the entire data set to find the anomaly. We identify the latitude and longitude of the location

of the highest positive relative vorticity anomaly at 850 hPa level in a rectangular box region where we expect the MD to be at its different phases (Day -1 to Day 2) and assign it as the location of the vortex center of the MDs at that phase. The latitude and longitude information as obtained from this procedure is compared with location information provided in the MAUSAM report for the verification purposes. Each depression was centralized to 0° latitude and 0° longitude. The horizontal distribution of relative vorticity anomaly and wind vector anomaly was plotted (not shown here) in the relative longitude - relative latitude coordinate to see if the circulation pattern is similar to that given for composite plots (Fig 4b and Fig 5a) of Hunt et al. (2016).

As a first step in analyzing different factors that may help to maintain the MD activity over land and its persistence, we check surface soil moisture data. Global Land Data Assimilation System (GLDAS-2.0, Rodell et al., 2004) daily data at 0.25° × 0.25° resolution was used for the study. GLDAS-2.0 contains soil moisture of the top layer (0-10cm) from Catchment Land Surface Model 3.6, and it only covers up to December 2014. Therefore, the soil moisture analysis is not performed for MD events after 2014. The 5.5° × 5.5° box around the center of the depression (identified in the tracking process mentioned earlier) on Day 2 (Day 0 being the land falling day) of each system is considered for the analysis. The soil moisture content above the Day 2 region (note that this region varies depending on the event) is determined from the day when the system is above this region (Day 2) to three days before the system passes through the region (marked by Day -1) for each MDs in TOP and BOTTOM cases. Soil moisture information in the rectangular box is centralized to 0° latitude, and 0° longitude while compositing. Composite plots for the BOTTOM and TOP cases are created separately, and then the contrast between them is depicted by subtracting the composite BOTTOM from the composite TOP.

Daily evolution (Day -3 to Day 2) of precipitation (IMD data) anomaly was separately plotted for TOP and BOTTOM cases to see whether any positive rainfall has occurred over the Gujarat region. If any rainfall is observed, to check whether it is due to MTC and to check if MTC is supporting the cyclonic circulation of the westward MD in any kind, a detailed analysis of the 20 MDs (TOP 10 and BOTTOM 10 cases) is conducted. For each case, relative vorticity anomaly ( $\times 10^{-5}\text{s}^{-1}$  - as color contour) and wind velocity

anomaly (as vectors) are plotted at 500hPa and 850 hPa. Analysis at the 500 hPa level is done to understand the process in the mid-troposphere where the mid-tropospheric cyclone (MTC) has maximum intensity. The 850 hPa level is plotted to see the MD location (MD location will be shifted at 500 hPa as it has a southwestward tilt with height) and to check whether there is any MTC-associated weak cyclonic vorticity at lower levels also. Relative vorticity, u wind velocity, and v wind velocity are taken from ERA-5 data, and anomalies are calculated with respect to the daily climatology constructed from 30 years of reanalysis data. Additionally, mid-tropospheric cyclonic circulations over the west coast of India around the region of Gujarat during the MD lifetime are identified from MAUSAM reports.

The anomaly of the Vertical Integral of divergence of moisture flux (VIDMF,  $\text{kgm}^{-2}$ ) is also estimated to show the locations of moisture convergence during each MD event period. The horizontal rate of moisture flow, per unit length across the flow, for a vertical column of air from the surface to the top of the atmosphere is the vertical integral of the moisture flux. The rate of moisture spreading outward from a place is its horizontal divergence. The variable is directly taken from the ERA-5 Reanalysis data. The daily data is constructed by taking the mean of 6 - hourly data, and the anomaly is calculated from daily climatology.

Relative vorticity at 10 pressure levels from 1000 hPa to 200 hPa (1000,850,700,600,500,400,350,300,250,200) are utilized to make vertical structures (pressure level vs relative longitude/latitude diagrams). Hovmoller diagrams are created with time on one axis (Day -5 to Day 5) and longitude on the other to depict the spatiotemporal variation of dynamic and thermodynamic fields such as relative vorticity and VIDMF (used anomaly from daily climatology for all the variables). The data has been averaged from 15-26°N to see longitudinal variations. Again, these meteorological parameters are obtained directly from the ERA-5 Reanalysis data.

# 3. Results and discussion

## 3.1 Mean statistics on frequency and duration of MDs

The frequency of MDs is found to be 2.4 per summer season (BOB depression-1.9, land depression-0.5). Individual MDs in July and August (Figure 2) follow a pattern that is fairly similar to the mean trajectory shown in the previous study of Sikka (1977). Figure 2 further shows that the spread in the tracks of MDs is greater in the months of June and September. i.e., individual tracks are well separated relative to other summer months. Despite the fact that our selection criteria are slightly different and we were unable to plot tracks of MDs whose location coordinates are not provided in the IMD reports,

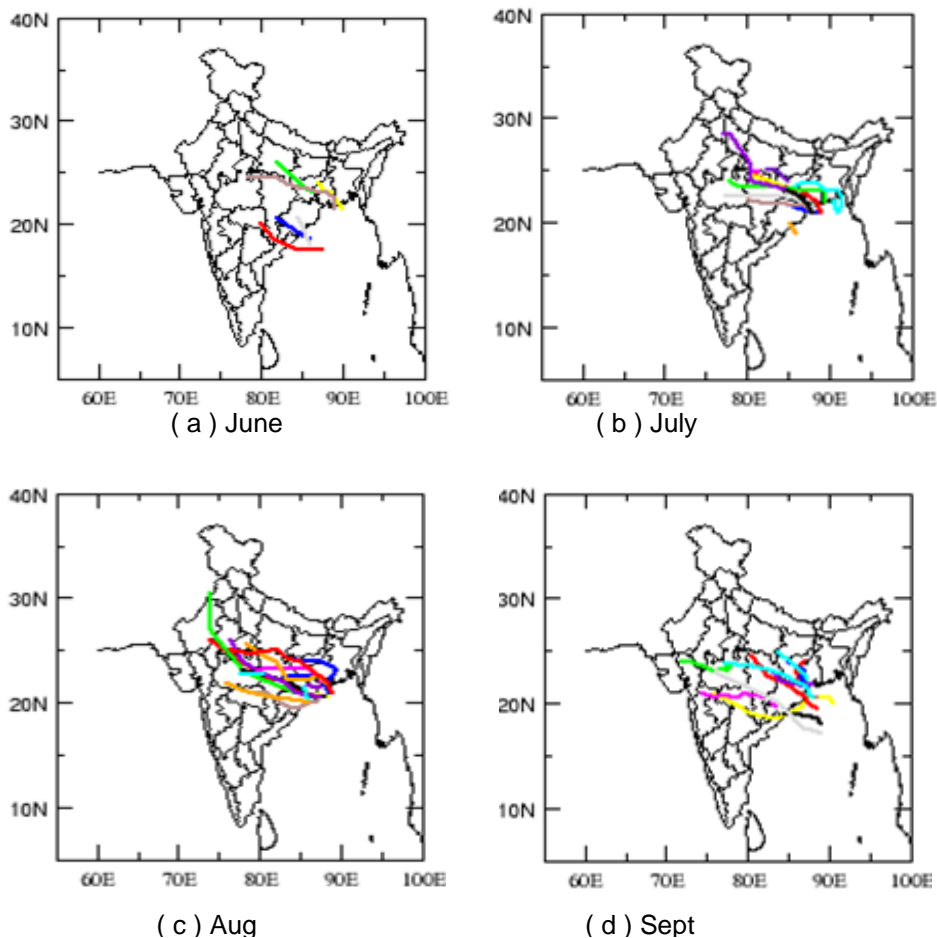


Figure 2. Tracks of MDs for (a) June, (b) July, (c) August, and (d) September

these month-wise behavioral inferences are consistent with Sikka (1977), who provided a thorough review of studies on statistics and characteristics of MDs. In July and August, there are more MDs than in June and September (Table 1). This agrees with Krishnamurthy and AjayaMohan's (2010) findings for the 1888–2003 study period. There is not much variation in the MD's average lifespan from one month to another.

*Table 1. Month Wise statistics of MDs for the period 1991-2020*

| Lifetime (days)                   | June | July | Aug | Sept | Total MDs                    |
|-----------------------------------|------|------|-----|------|------------------------------|
| 2                                 | 3    | 4    | 5   | 6    | 18                           |
| 3                                 | 5    | 7    | 4   | 4    | 20                           |
| 4                                 | 2    | 2    | 10  | 2    | 16                           |
| 5                                 | 1    | 3    | 3   | 3    | 10                           |
| 6                                 | 0    | 1    | 0   | 0    | 1                            |
| 7                                 | 0    | 0    | 0   | 0    | 0                            |
| 8                                 | 1    | 1    | 0   | 0    | 2                            |
| 9                                 | 1    | 0    | 0   | 0    | 1                            |
| Total                             | 13   | 18   | 22  | 15   | 68                           |
| Mean lifetime of MD in each month | 3.9  | 3.7  | 3.5 | 3.1  | Average duration of MDs =3.5 |

MDs with the shortest lifespans last around two days and the climatological life expectancy of MDs is estimated to be 3.5 days (Figure 3) and almost equal to Hunt et al. (2016a; 3 days). MDs can even last up to 9 days, but are less frequent. The mean distance covered by the MDs after landfall is 660 km with a maximum value of 1693 km and a minimum of 21 km (Figure 4). According to Kishtawal et al. (2013), the mean IPL of wet state MDs (101 cases) and dry state MDs (95 cases) was 820 km, and 541 km,

respectively for their analysis period. So, if we estimate the mean for the entire sample (196 cases), it is around 680 km, which is very close to the mean IPL of our sample.

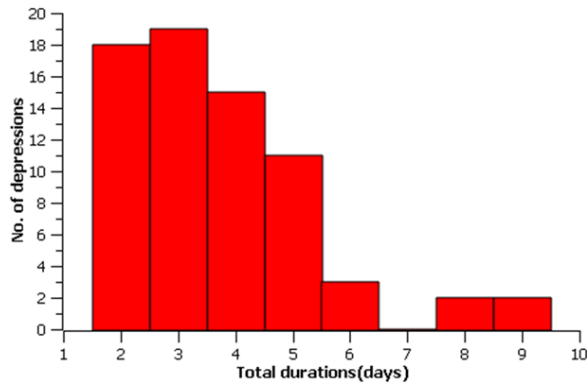


Figure 3. Lifetime statistics of MDs during the boreal summer monsoon season of 1991-2020 (30 years)

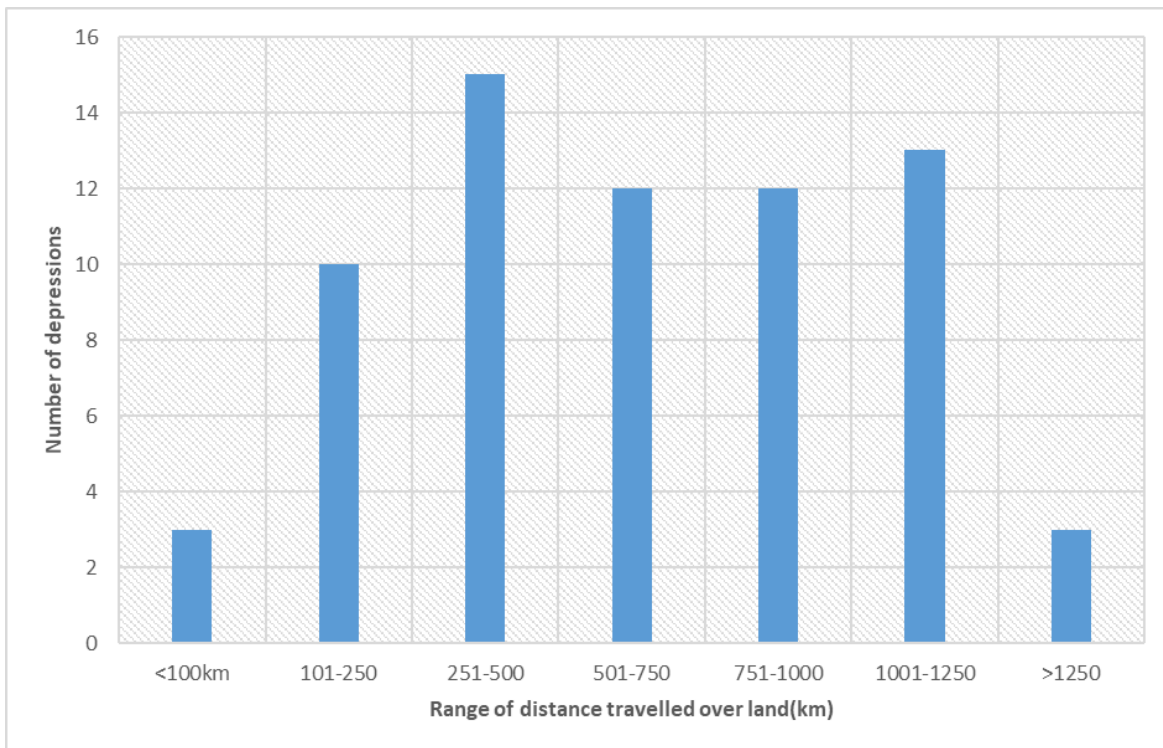


Figure 4. A bar diagram showing how far the MDs can travel over land after hitting the coastline and the number of MDs for each range of inland penetration lengths for the period 1991-2020.

### 3.2 Spatio-temporal analysis of anomalous precipitation and selection of long-lived and short-lived MDs

Figure 5(a) shows precipitation anomaly during depression days (a composite of 70 events - 274 depression days) in which Orissa and nearby states have the highest positive anomaly values. This is because the coastal regions of BoB usually experience substantial rainfall from all coastline-crossing MDs, regardless of their lifespan and distance traveled across land. On days of MD, orographic rainfall over the Western Ghats is also amplified, since the presence of far-off storms intensifies the circulation (Krishnamurthy and AjayaMohan, 2010). But a reduction in rainfall is observed over Northeast India. There is a secondary rainfall maximum over central India, covering much of the Madhya Pradesh state which is also equally important (compared to the rainfall maximum in the coastal regions) as it can cause large-scale floods thus adversely impacting life and property. The filtering process of depression days having extreme rainfall over this region bounded by latitudes, 20 to 25°N, and longitudes, 73 to 81°E yielded 54 depression days corresponding to 30 MD events. Figure 5(b) is a composite of precipitation anomalies for those cases and it confirms the validity of our selection criteria. As heavy precipitation occurs in the vicinity of the MD propagation path, these 30 MDs are most likely the systems that followed the mean MD track and intruded farther into the land.

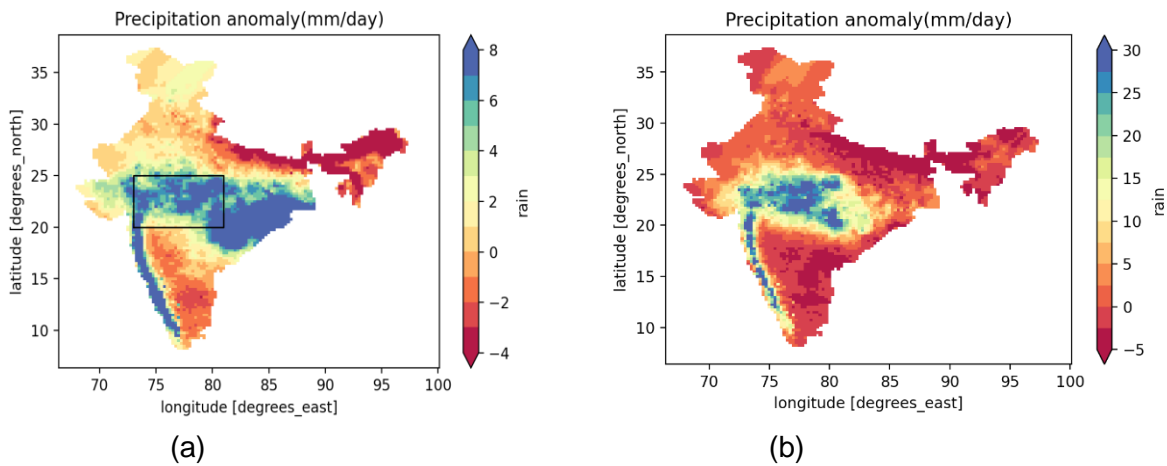


Figure 5. (a) Composite plot for precipitation anomaly for depression days  
(b) Composite plot for depression days which caused extreme rainfall events over central India bounded by the coordinates 20-25°N latitudes and 73-81°E longitudes

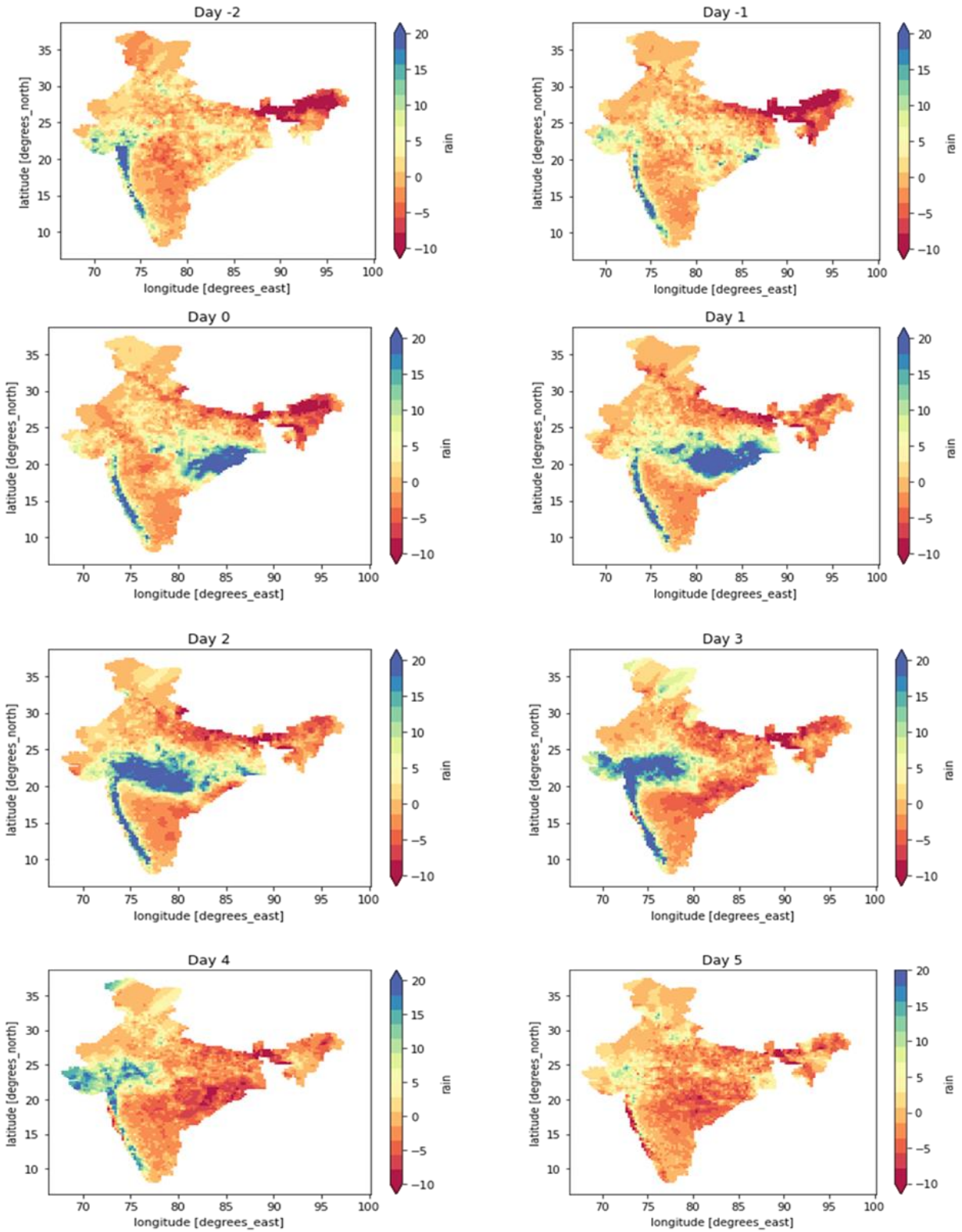


Figure 6. The daily evolution of anomalous precipitation for 21 MD events that caused extreme rainfall over central India (20 - 25°N and 73-81°E)



Figure 6 shows the composites of the daily evolution of anomalous precipitation (mm/day) of 21 MDs that are remaining after discarding 7 land depressions and 2 exceptional cases from the 30 selected MDs (reasons for removing the events are described in the data and methods section). Day 0 is assigned to be the landfall day of each MD event. There is no obvious rainfall anomaly over land prior to the landfall (designated by Day -2, -1) since precipitation will be concentrated more over BoB. The evolution of rainfall anomalies is west-northwest from Day 0 to Day 3 as consistent with earlier studies (e.g., Sikka 1977). The systems began to deteriorate on Day 4 and gets fully dissipated by Day 5. According to statistics (table is not shown here), the extreme rainfall over central India occurs on average two days after it crosses the coastline (on Day 2). The rainfall anomaly in Figure 6 is also greater over central India on Day 2.

*Table 2. List of the TOP 10 MDs, their inland penetration lengths (IPL), and the dates of Northeastern Arabian Sea MTC, if any occurred during the lifetime of MD*

| MD events                 | IPL (Km) | Mid-tropospheric cyclonic circulation             |
|---------------------------|----------|---|
| <b>5-8 Aug 2007</b>       | 1086     | July 31- Aug 07                                   |
| 29 Aug-1 Sept 2006        | 1216     | Aug 29- 30  |
| <b>2-5 July 2006</b>      | 925      | June 28- July 04                                  |
| <b>12-16 Sept 2005</b>    | 1220     | Cyclonic circulation at lower and mid-troposphere |
| <b>30 July-1 Aug 2013</b> | 953      | Cyclonic circulation at lower and mid-troposphere |
| <b>4-9 July 2007</b>      | 1197     | Cyclonic circulation at lower and mid-troposphere |
| <b>27-31 July 1991</b>    | 1034     | July 27-30  |
| 16-20 Aug 2016            | 1271     | Aug 18-19   |
| <b>6-9 Aug 2019</b>       | 1042     | Aug 3-7 & Aug 7-9                                 |
| 16-23 June 2011           | 1114     | June 20-23  |

*Table 3. List of BOTTOM 10, their inland penetration lengths (IPL), and the dates of Northeastern Arabian Sea MTC, if any occurred during the lifetime of MD*

| MD events              | IPL (Km) | Mid-tropospheric cyclonic circulation |
|------------------------|----------|---------------------------------------|
| <b>22-23 Sept 2011</b> | 128      | -                                     |
| 20-21 July 2009        | 246      | July 10-19                            |
| <b>27-28 Aug 2003</b>  | 155      | -                                     |
| <b>16-17 Sept 1995</b> | 278      | -                                     |
| <b>28-30 Sept 2006</b> | 21       | -                                     |
| <b>7-8 Aug 2018</b>    | 115      | -                                     |
| 18-19 July 2017        | 30       | -                                     |
| 20-22 June 2015        | 130      | -                                     |
| <b>26-28 Sept 1995</b> | 273      | -                                     |
| <b>21-22 Sept 1991</b> | 100      | -                                     |

Among the 21 events, 10 MDs that traveled large distances over the Indian landmass are characterized as TOP cases. Among all the 56 BoB MDs, 10 systems that traveled the shortest distances over land are classified as BOTTOM cases. Selected cases (column 1) as intruding into the landmass are listed in Tables 2 and 3. We have also included the approximate straight-line distance as covered (i.e., IPL) by each system after crossing the coastline (column 2) but before getting dissipated over the Indian continent. TOP cases of MDs have IPL greater than 900 Km, while BOTTOM cases of MDs have IPL less than 300 Km.

### 3.3 Soil moisture analysis

Since we have soil moisture data only till 2014, 3 MDs in the list of BOTTOM cases and 2 MDs in the TOP list which are formed after 2014 are not currently included in the soil moisture analysis. Because soil moisture is a land-only parameter, a rectangular box around the vortex center contains a small portion of the oceanic region sometimes. If we include such cases while compositing, information from the rest of the MDs in that portion will vanish in the final figure (since taking mean requires values in all cases). We avoid this situation by removing such cases for creating composite plots. Hence, we are left with 5 MDs from the TOP list and 5 MDs from the BOTTOM list.

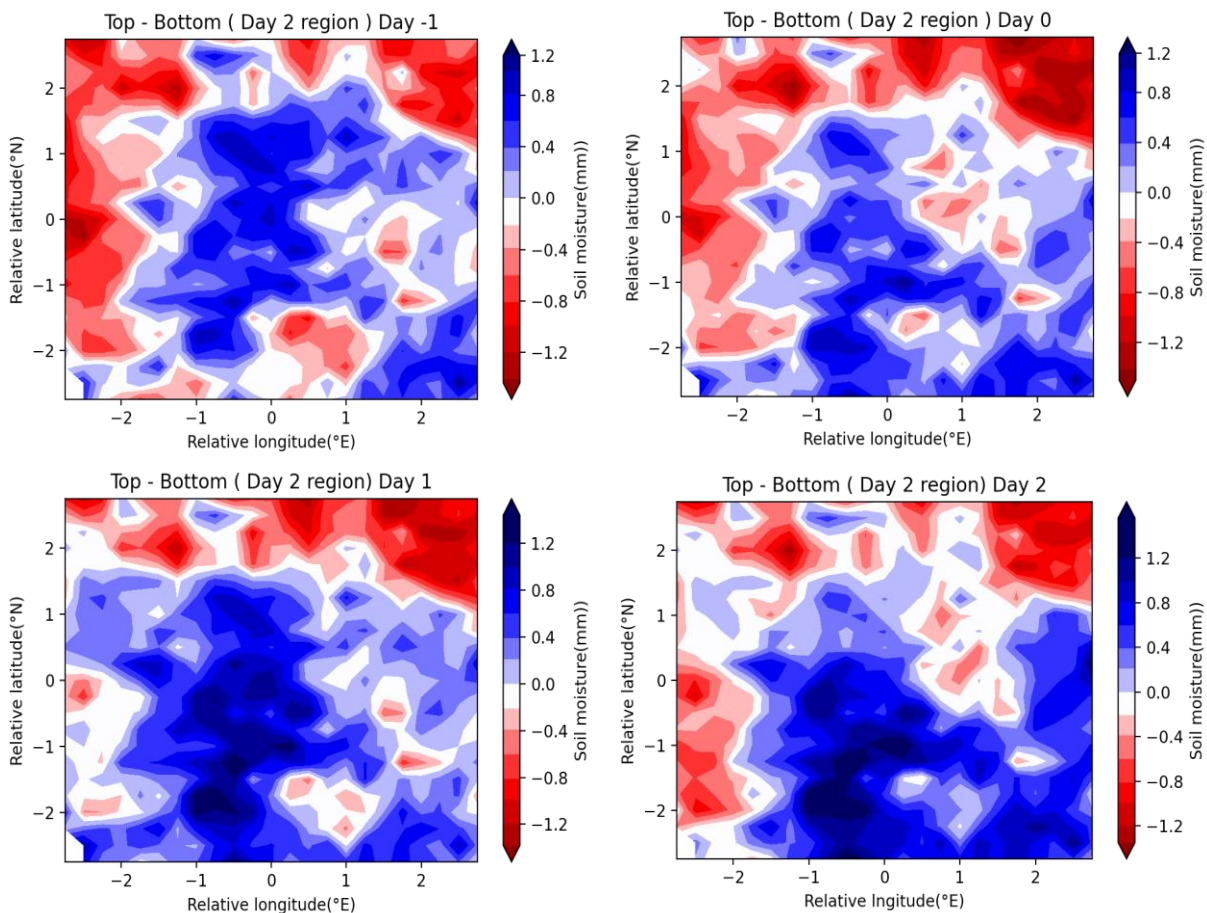


*Figure 7. The relative longitude-latitude plot of contrast between the TOP and BOTTOM soil moisture content above the Day 2 region from Day 2 to Day -1. The coordinate origin is centered with respect to relative vorticity maxima*

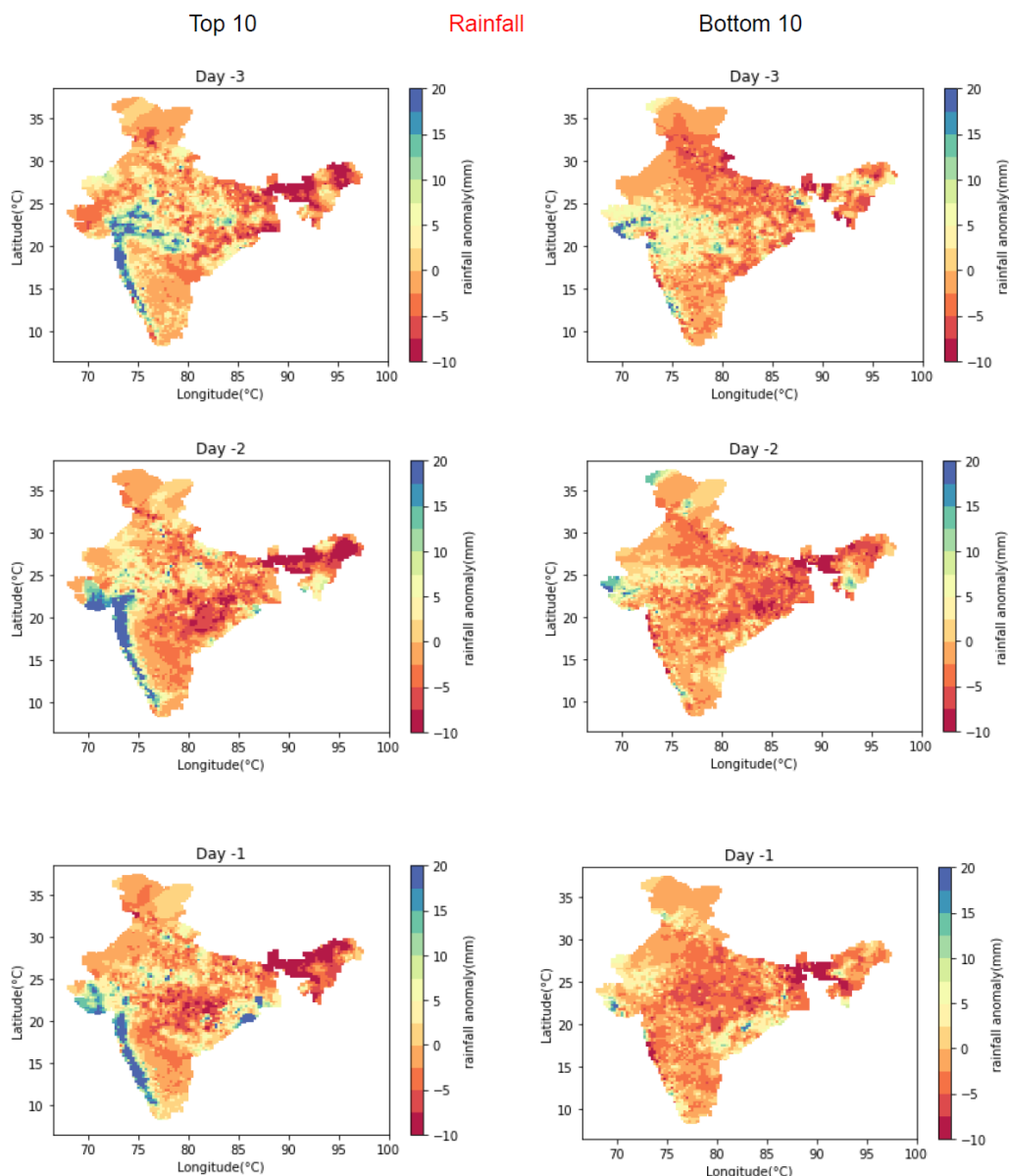
Earlier studies looked at ground wetness conditions of the entire monsoon core zone before each MD formation. However, soil moisture is a very local surface parameter and if it has any influence on MD, we expect it to be on a local scale. Since different MDs are traveling in different paths, for each MD, we focused only on a square box of dimension  $5.5^\circ$  with the center as the location of the MD after 2 days of landfall. From the day when the MD is exactly over the selected region, we trace back to three days before that day and find the difference between soil moisture content (spatial distribution) for MDs with larger inland penetration (TOP cases) and MDs with shorter inland penetration length (BOTTOM cases). In other words, the contrast between the TOP and BOTTOM soil moisture content above the region around the center of the MD on Day 2 of each system ('Day 2 region') is analyzed (Figure 7) from Day 2 back to Day -1 (Day 0 is the landfall day). By doing this, we are considering the diversity in MDs' track thus facilitating us to look at more regional influences. Note that x and y axis denote relative longitude and relative latitudes, respectively since each MD was centralized to  $0^\circ$ latitude,  $0^\circ$ longitude while compositing.

Figure 7 effectively shows positive soil moisture anomaly for the TOP cases in all the phases. The absolute value of soil moisture ranges from 0 to 8 over different parts of the monsoon core region at different times, and the mean value falls in the range of 5-6. Hence even an anomaly of magnitude 0.3 is statistically significant. Even though more quantitative analyses are required, our result implies that, in comparison to short-lived MDs, long-lived MDs had higher soil wetness over the region ahead of the MD. So, soil moisture can be considered one of the driving factors that aid in the maintenance of MD activity and allows it to penetrate deeper into the land before dissipation. Therefore, our result demonstrates a link between soil moisture and landfalling MD activity, which is consistent with Kishtawal et al. (2013).

The primary difference between our study and that of Kishtawal et al. (2013) is that they used antecedent rainfall as a surrogate for ground wetness, which will only contain the in-situ source of moisture. Whereas, we used soil moisture data itself, which includes both in-situ sources like precipitation and advected moisture content from remote sources like that brought in by winds from the Arabian Sea and BoB.

### 3.4 Relation of MTC to long-lived and short-lived MDs

Daily evolution of precipitation anomalies is analyzed for composites of TOP and BOTTOM cases. In the TOP case (Figure 8(a)), we can see a large positive rainfall anomaly over the western coast of India on days prior to landfall of MD, whereas in the case of BOTTOM events (Figure 8(b)), such precipitation anomaly is not observed. According to Miller and Keshavamurthy (1968), MTCs must be the primary activators and regulators of rain across western India.



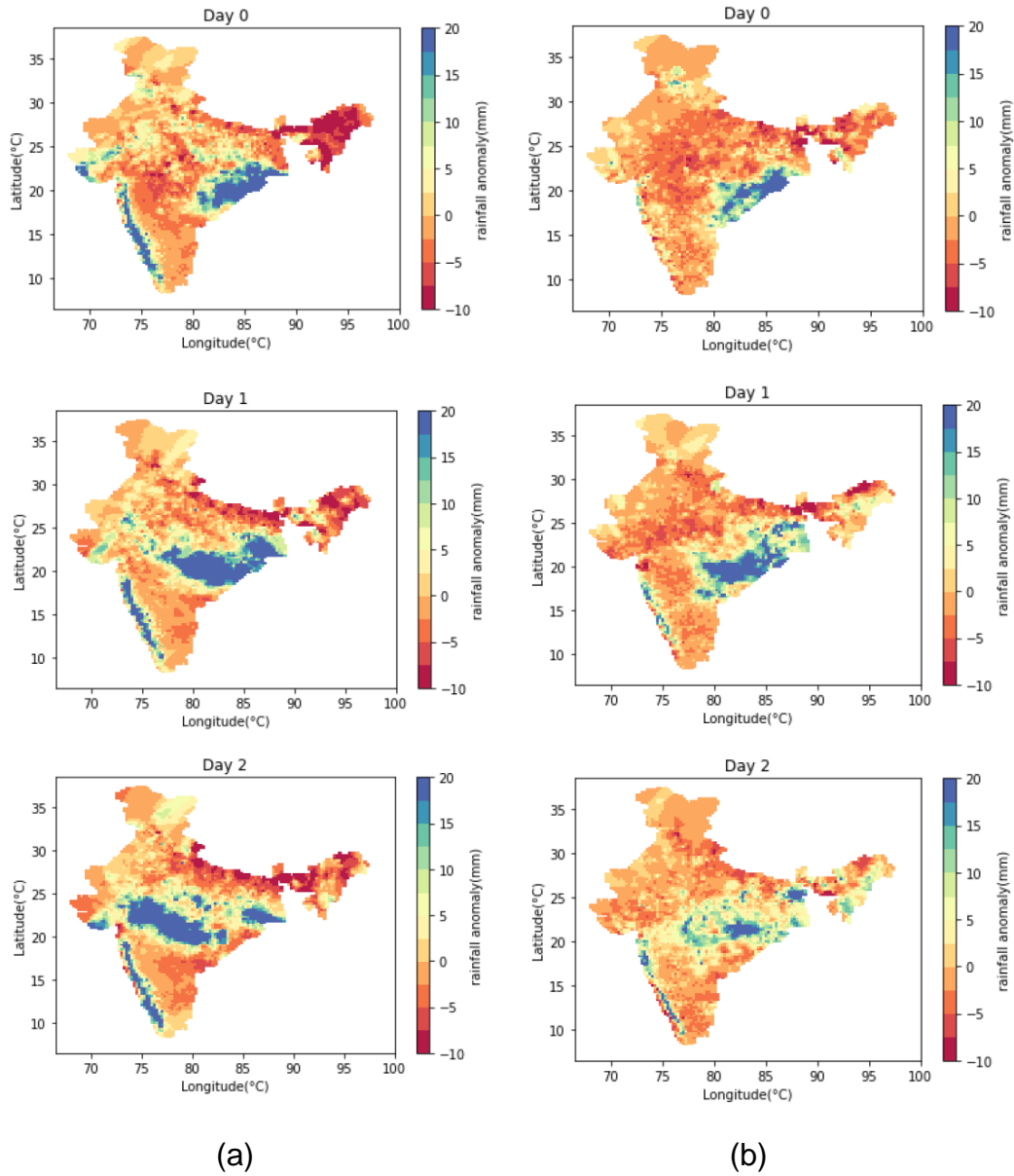
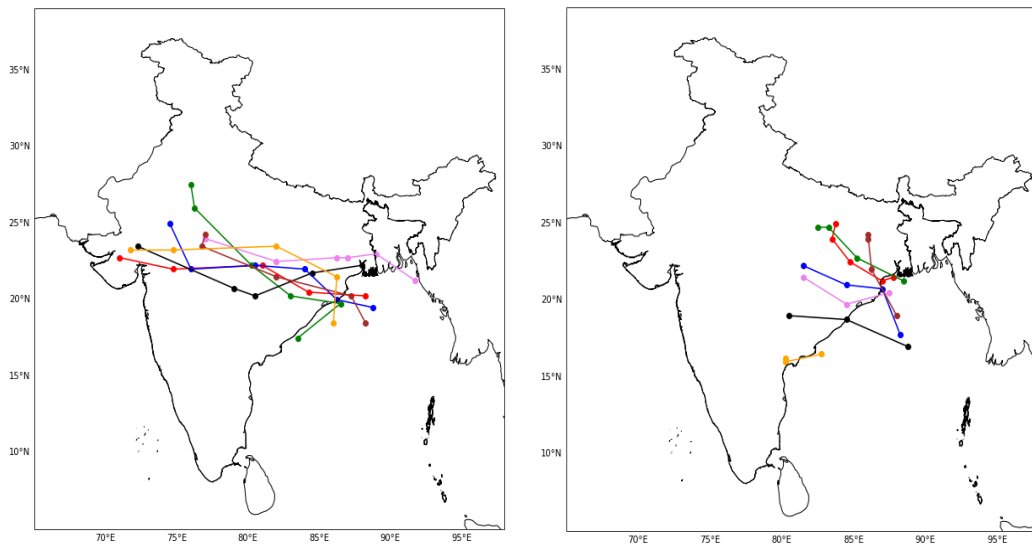


Figure 8. A composite of the daily evolution of precipitation anomaly for (a) TOP (left panel) and (b) BOTTOM (right panel) cases

Interestingly, in all the 10 cases of TOP MDs, there is a consistent presence of mid-tropospheric cyclonic vorticity prior to or during the period of the MD (Table 2). Whereas only 1 MD is accompanied by MTC in the BOTTOM group (out of 10 BOTTOM cases). This is a clear indication that the presence of mid-level cyclonic vorticity creates some environment conducive to the long-distance propagation of MDs and their subsequent persistence along the Indian subcontinent.

Hereafter, while creating composite plots for TOP and BOTTOM cases, we choose 7 cases (as highlighted in bold letters in [Table 2&3](#)) out of the 10 cases from each group that have similar spatiotemporal patterns of meteorological parameters. The corresponding tracks produced using the relative vorticity field at 850 hPa level for the selected cases are shown in [Figure 9](#).



*Figure 9. Tracks of MDs with 850 hPa relative vorticity anomaly maxima as the storm center for (a) TOP cases (b) BOTTOM cases*

In composites of TOP cases ([Figure 10](#)), from Day -3 onwards there is a presence of positive relative vorticity anomaly at 500 hPa over the Northeast Arabian Sea and neighboring northwest Indian region. From Day -3 to -1, the low-pressure system over the North Bay of Bengal (BoB) is gaining strength thus quickly transitioning into a MD. During this time period, the relative vorticity plot is showing co-existence of Arabian sea MTC and BoB MD. Moving in a westward direction, the MD crosses the eastern Indian coastline on Day 0. After that, both cyclonic circulations start interacting with each other while the MD is propagating towards the west. On Day 2, [Figure 10](#) shows a large area of positive vorticity spreading central to northwest India. The system starts dissipating on Day 3.

The daily evolution of relative vorticity anomaly shows similar patterns at 850 hPa pressure level also ([Figure 11](#)). However, the positive relative vorticity over Northwest India is extended over a larger area with less magnitude compared to the 500 hPa level, which gets more prominent by Day -1. This may be considered as MTC-induced cyclonic

vorticity at the lower troposphere. In other words, this can be interpreted as inducing lower-level cyclonic circulation under the influence of mid-tropospheric cyclones. When MD is moving westward, a merging of east-west vorticities occurs.

Figure 12 shows the composites of the vertical integral of moisture flux divergence for TOP cases. When moisture is dispersing or diverging, this parameter is positive; when moisture is concentrating or converging, it is negative (convergence). As a result, this component reveals whether atmospheric motions work to enhance (for convergence) or reduce (for divergence) the vertical integral of moisture.

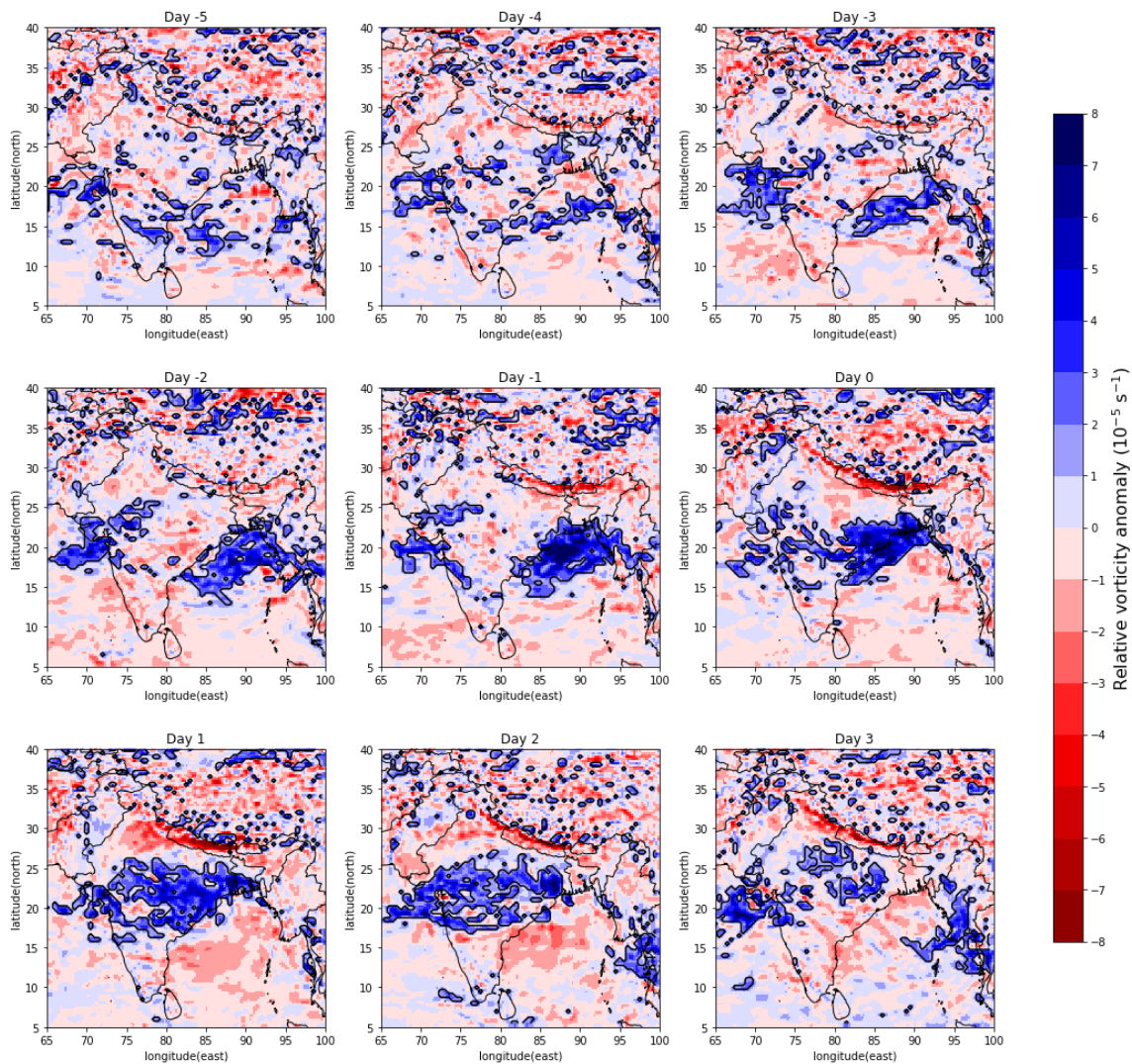


Figure 10. Composites of the horizontal pattern of relative vorticity anomaly at 500 hPa pressure level from Day -5 to Day 3 (Day 0 being the landfall day) for TOP cases



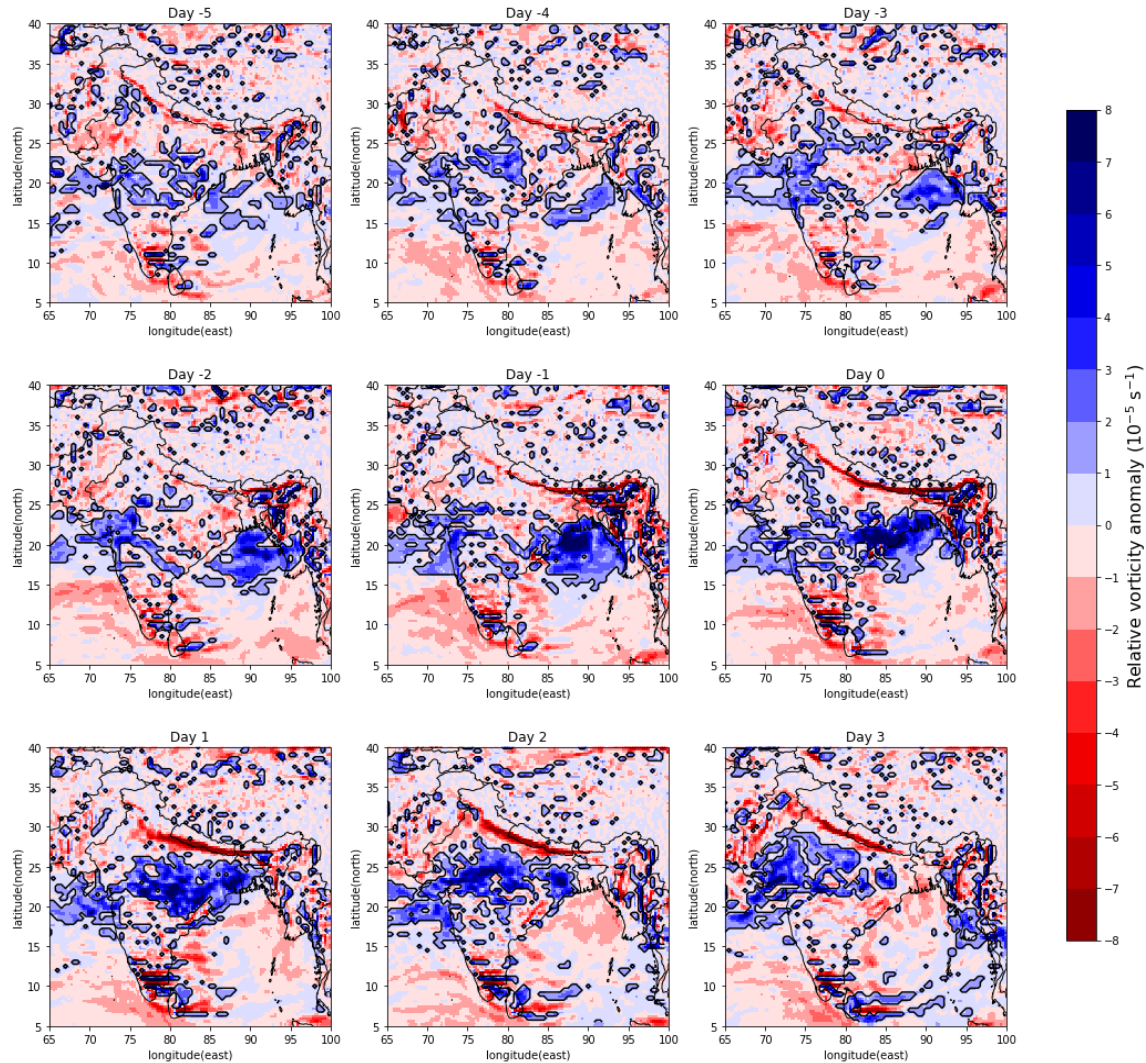


Figure 11. Composites of the horizontal pattern of relative vorticity anomaly at **850 hPa** pressure level from Day -5 to Day 3 for **TOP** cases

Water vapor is concentrated (negative values in the figure) toward the north BoB, the northeast Arabian sea, and the adjoining northwest Indian region, relative to the daily climatology of each region. Cyclonic vorticity associated with MTC might be bringing a large amount of moisture from the northeast Arabian sea. As moisture availability is increased in the atmospheric column ahead of the MD, the system probably gets intensified and travels longer over land.

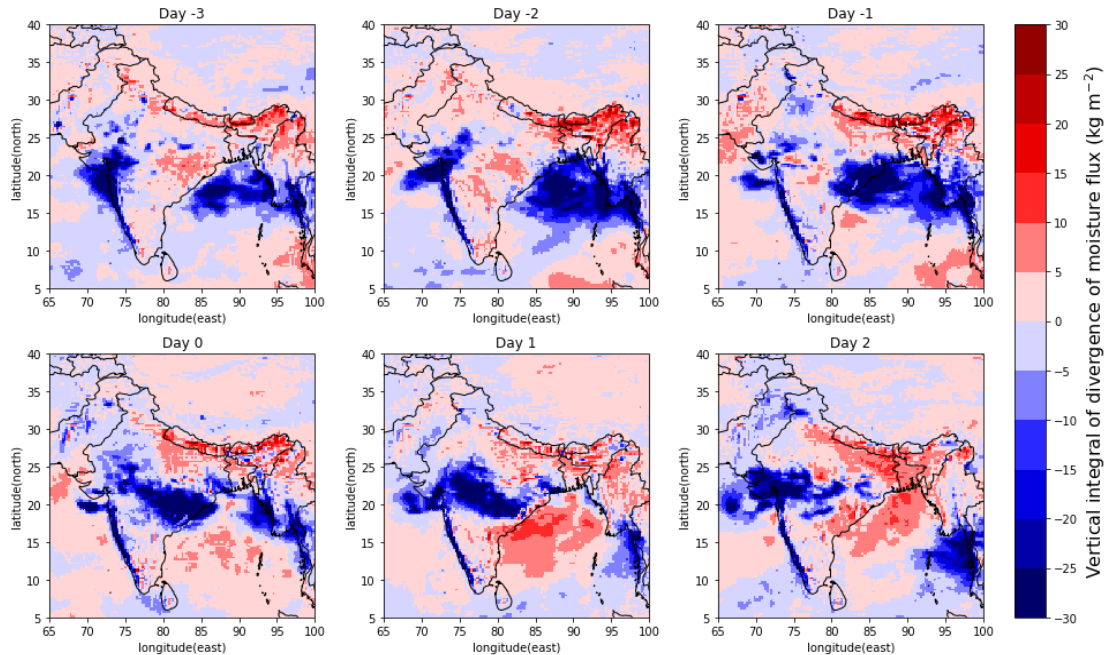


Figure 12. Composite of the evolution of vertical integral of divergence of moisture flux ( $\text{kgm}^{-2}$ ) over Indian region from Day -3 to Day 2 for **TOP** cases.

To illustrate the distribution of dynamic fields (wind vector, relative vorticity, VIDMF) for MTC-associated MDs, one typical example (2007 August 5-8) from the TOP list is selected. On Day -3 at 500 hPa (Figure 13(a)), the North-Eastern Arabian Sea had modest cyclonic vorticity, which on Day -2 became stronger. At the same time, MD over BoB gained strength and headed westward on Day -1. On Day 0 (i.e., when it crossed the Indian coastline) and afterwards, interestingly one can see the merging of these 2 cyclonic disturbances (one over northwest and the other over BoB) thus eventually forming a single intensified cyclonic circulation.

There is only weak cyclonic vorticity at 850 hPa pressure level (Figure 13(b)) over the Northeastern Arabian Sea, indicating that the system was an MTC (MTC has maximum vorticity at mid-troposphere with very weak vorticity at lower levels). MD moved towards the location of MTC (westward) rather than moving in a northwestward path. As expected, the VIDMF anomaly (Figure 14) is highly negative over Northwest India, indicating the occurrence of moisture convergence over the region during this period.

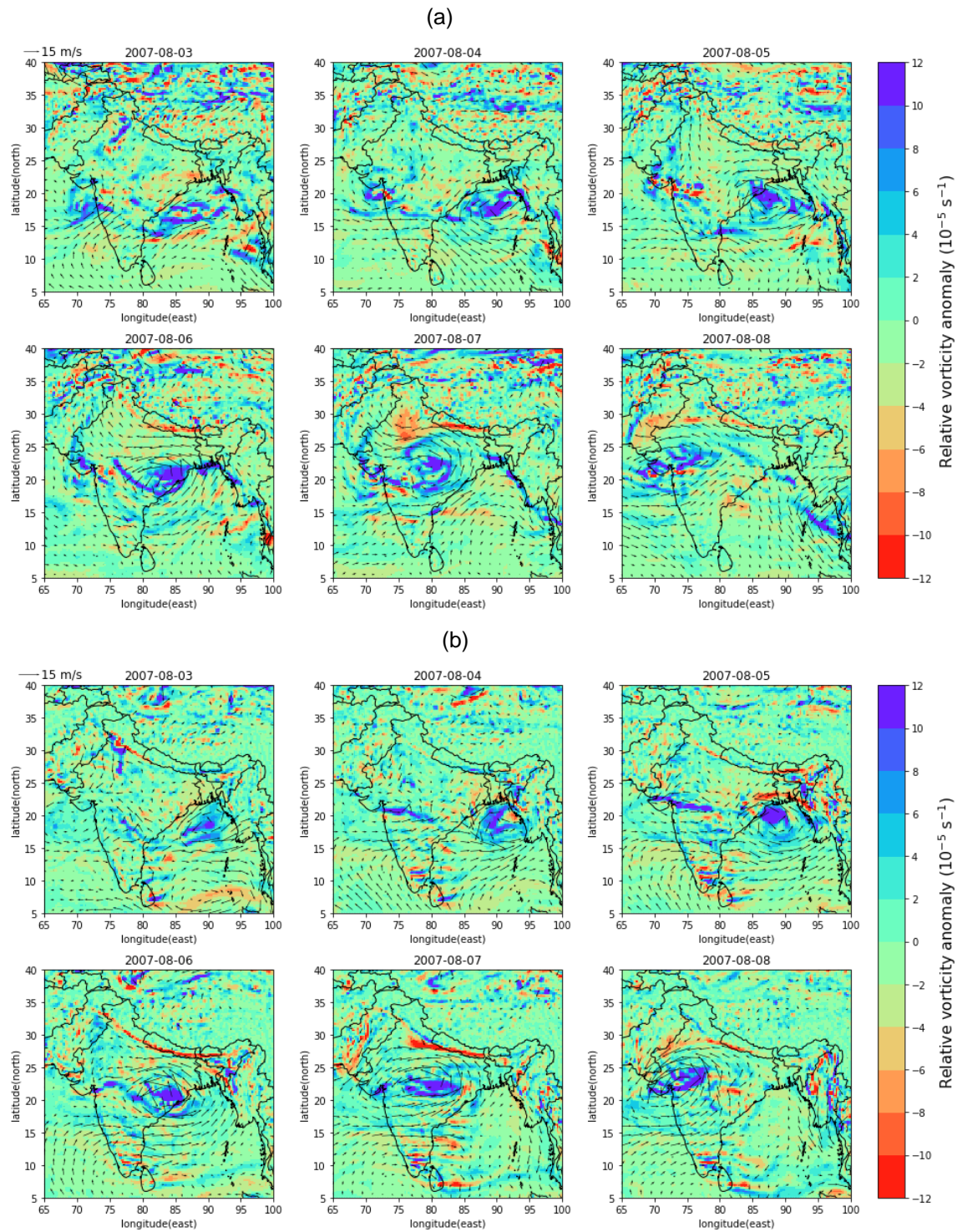


Figure 13. Horizontal pattern of relative vorticity anomaly (shaded) and wind velocity anomaly (vectors) from Day -3 to 2 (2007-08-06 - landfall day) for an MD during 2007 Aug 5-8 (an example from the TOP list) at (a) 500 hPa, and (b) 850 hPa

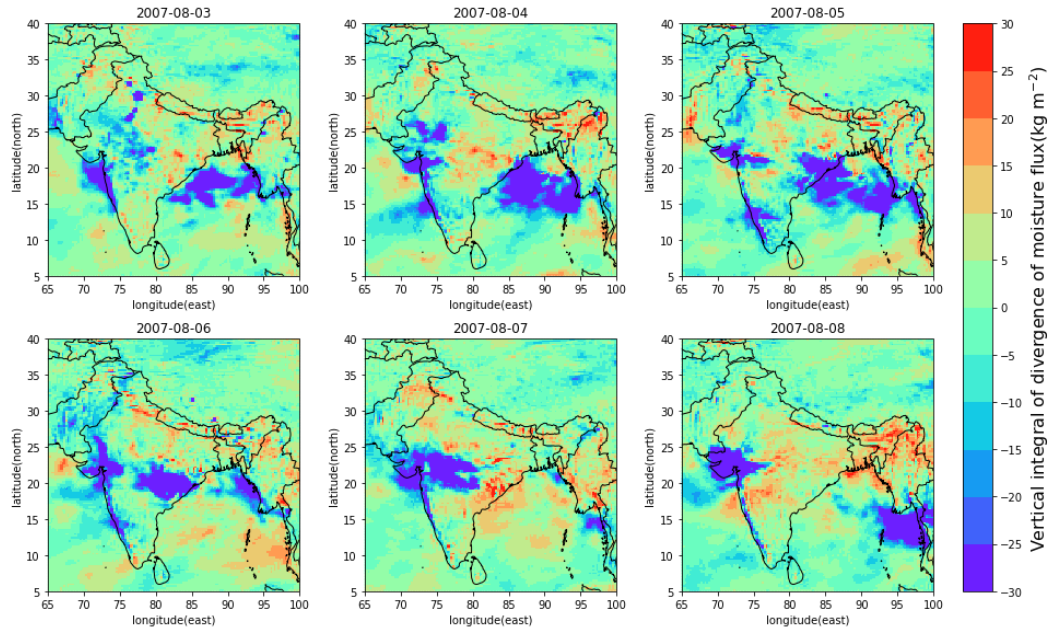


Figure 14. Horizontal pattern of VIDMF anomaly from Day -3 to 2 (2007-08-06 - landfall day) for MD during 2007 Aug 5-8 (an example from TOP list)

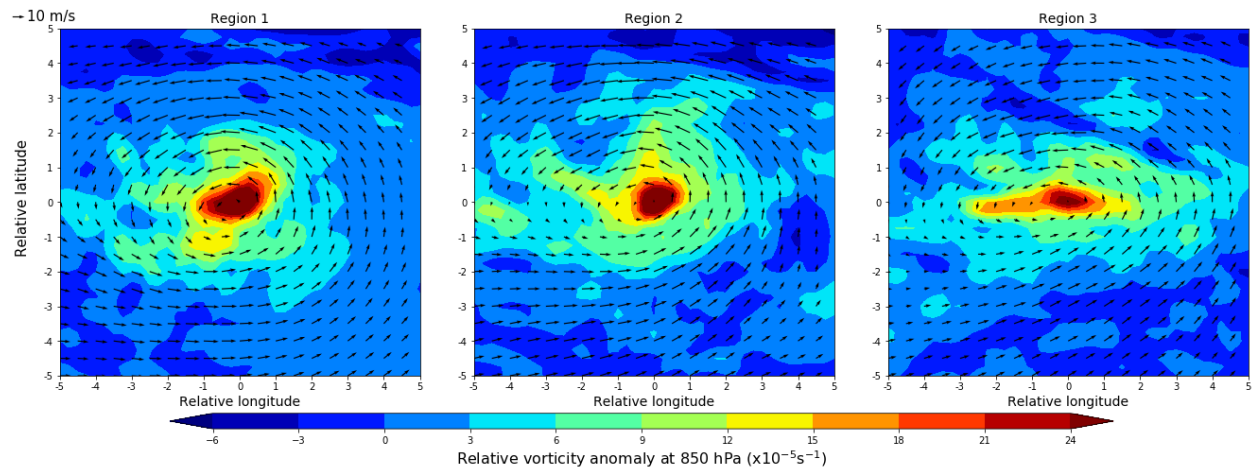


Figure 15. Storm-centered horizontal composite plots of relative vorticity anomaly at 850 hPa for TOP case. Regions are categorized according to when and where they fall within a specific longitudinal range.

|                    |                    |                    |
|--------------------|--------------------|--------------------|
| Region 1: 83-87° E | Region 2: 80-82° E | Region 3: 74-79° E |
|--------------------|--------------------|--------------------|

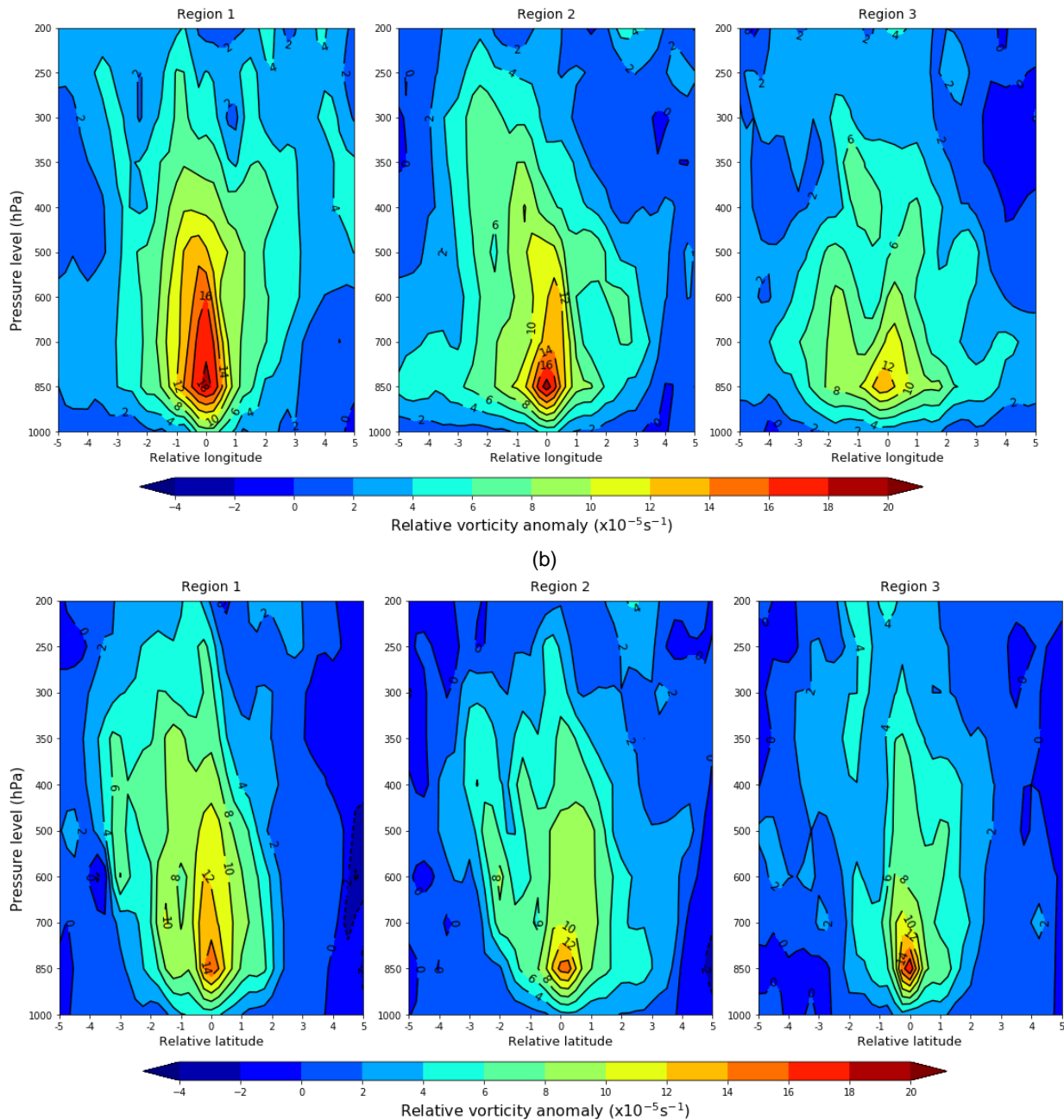


Figure 16. Storm-centered vertical composite plots of relative vorticity anomaly at different pressure levels for the TOP case. (a) latitudinal cross-section (b) longitudinal cross-section

Storm-centered composite plots of TOP group MDs are prepared next for more robustness of the results which also show similar patterns for relative vorticity and wind vectors as observed in the above case study. When the systems are in the eastern coastal region of India (Region 1), the horizontal composite at 850 hPa (Figure 14) exhibits symmetric circulation around its core and a nearly circular wind pattern. When the system

moves more into the land (Region 2) the symmetric pattern is slightly deforming, particularly on the westward side. In region 3, the system has contracted latitudinally and stretched longitudinally, forming an elliptical structure. These structural changes are also confirmed by storm-centered vertical composites (Figure 16). Figure 16(a) illustrates an increase in longitudinal extent in region 3 and Figure 15(b) indicates a reduction in latitudinal extent.

Figures 17-19 further ascertain our results by examining the BOTTOM cases, as all the plots considerably differ from the TOP cases. In 500 hPa composites BOTTOM cases (Figure 17), there is not much positive relative vorticity anomaly over Northwest India from Day -5 to Day 3. At 850 hPa level (Figure 18), central and western India even have slight anticyclonic behavior.

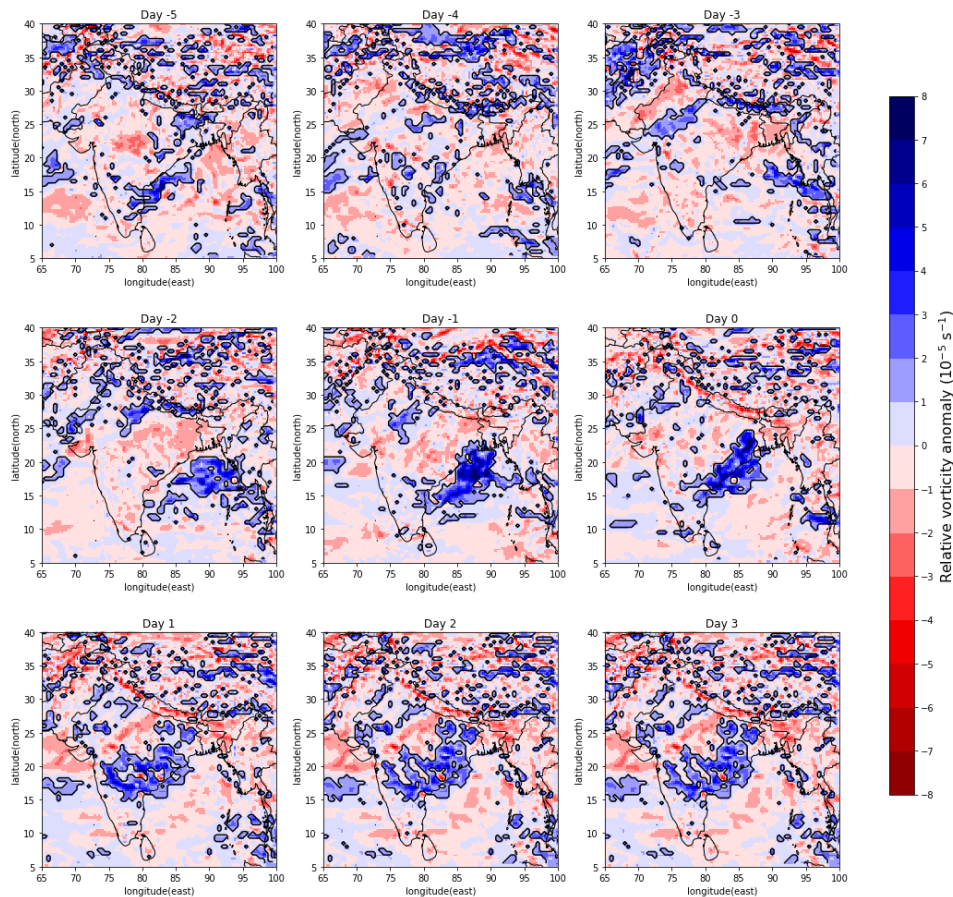


Figure 17. Composites of the horizontal pattern of relative vorticity anomaly at 500 hPa pressure level from Day -5 to Day 3 for **BOTTOM** cases

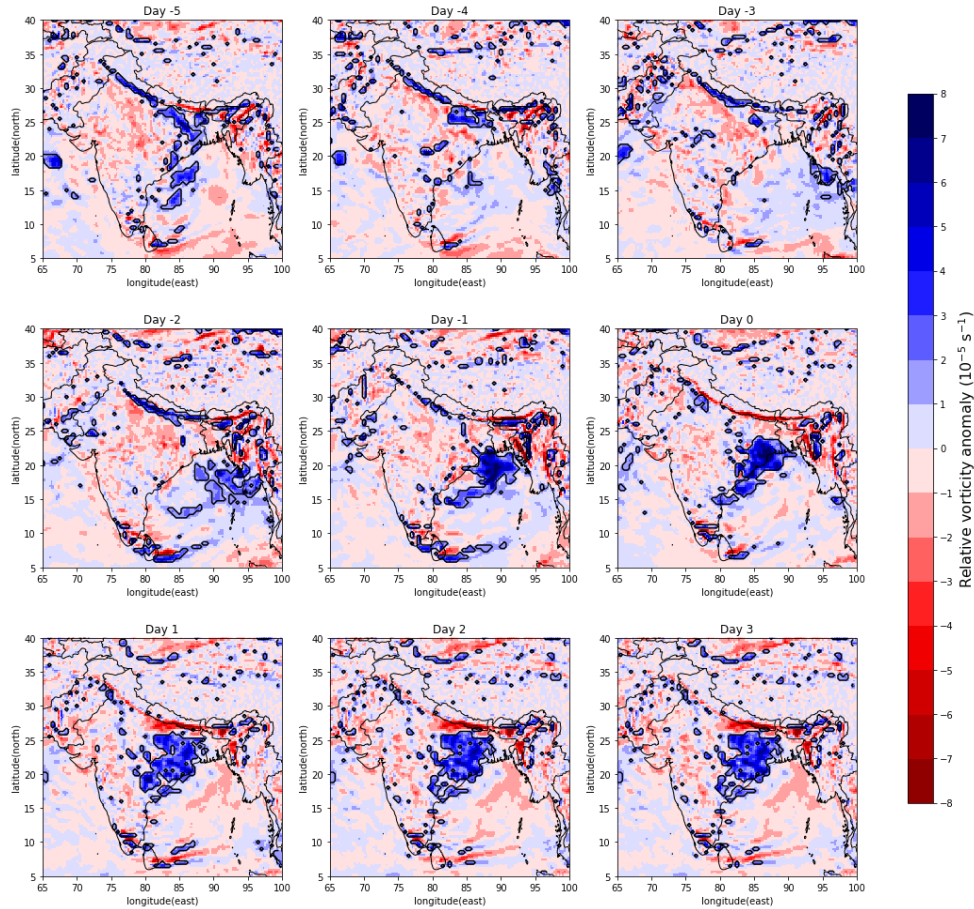


Figure 18. Composites of the horizontal pattern of relative vorticity anomaly at 850 hPa pressure level from Day -5 to Day 3 for **BOTTOM** cases

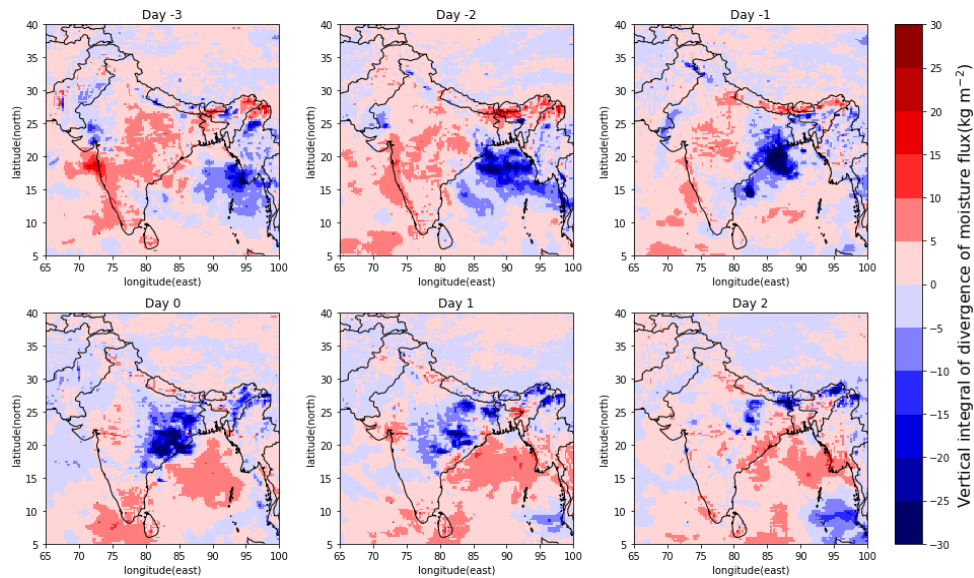


Figure 19. Composite of the evolution of vertical integral of divergence of moisture flux ( $\text{kgm}^{-2}$ ) over Indian region from Day -3 to Day 2 for **BOTTOM** cases.

Anticyclonic wind (with Northwest India and central India showing divergent centers of moisture) is expected to bring dry air to central India, thus creating background moisture conditions unfavorable for the sustenance of MD structure which results in the rapid dissipation of MD thus limiting its progression into the Indian landmass.

To show further the results, the circulation pattern for the BOTTOM events, the 2011 Sept 22-23 case is selected. At 500 hPa (Figure 20(a)), wind vectors over Gujarat and Rajasthan show an anticyclonic behavior (not exactly a closed circulation) which may cause dry air intrusion from heat low over Rajasthan and Pakistan region. Also, there is no sign of wind flow from the Arabian sea towards the area of the usual MD propagation path, especially post-landfall (2011-09-22 onwards). At 850 hPa level (Figure 20(b)), starting from a latitude of 30°N to 15°N, a large area of the Indian landmass centered nearly about 80°E has northeasterly wind flow. This pattern is not observed in the TOP case. In the VIDMF anomaly for the BOTTOM case (Figure 21), there is an absence of negative anomaly over western India which was present in the TOP case (Figure 14). The difference between them is also depicted using Figure 22. While the systems in the TOP list moved in a west-northwest direction, the BOTTOM cases seem to have a less westward component in their propagation velocity and moved in a northwest direction. We attribute this difference in propagation direction to the absence of MTC over Northwest India in the BOTTOM cases. However, the exact mechanism through which MTC affects MD propagation along the Indian landmass is still not clear and it is a subject which requires more careful analysis and is beyond the current work.

The Hovmöller diagrams at both lower and mid-level troposphere for the relative vorticity anomaly field are significantly different for TOP and BOTTOM group MD composites (Figure 23). In the BOTTOM case, positive relative vorticity that is most probably associated with MDs only propagates around 80°E, whereas it goes beyond 70°E for the TOP composite at both pressure levels. This comprehensively demonstrates the reliability of our categorization of TOP and BOTTOM MD groups (as done in Tables 1-2) based on the IPL as estimated.



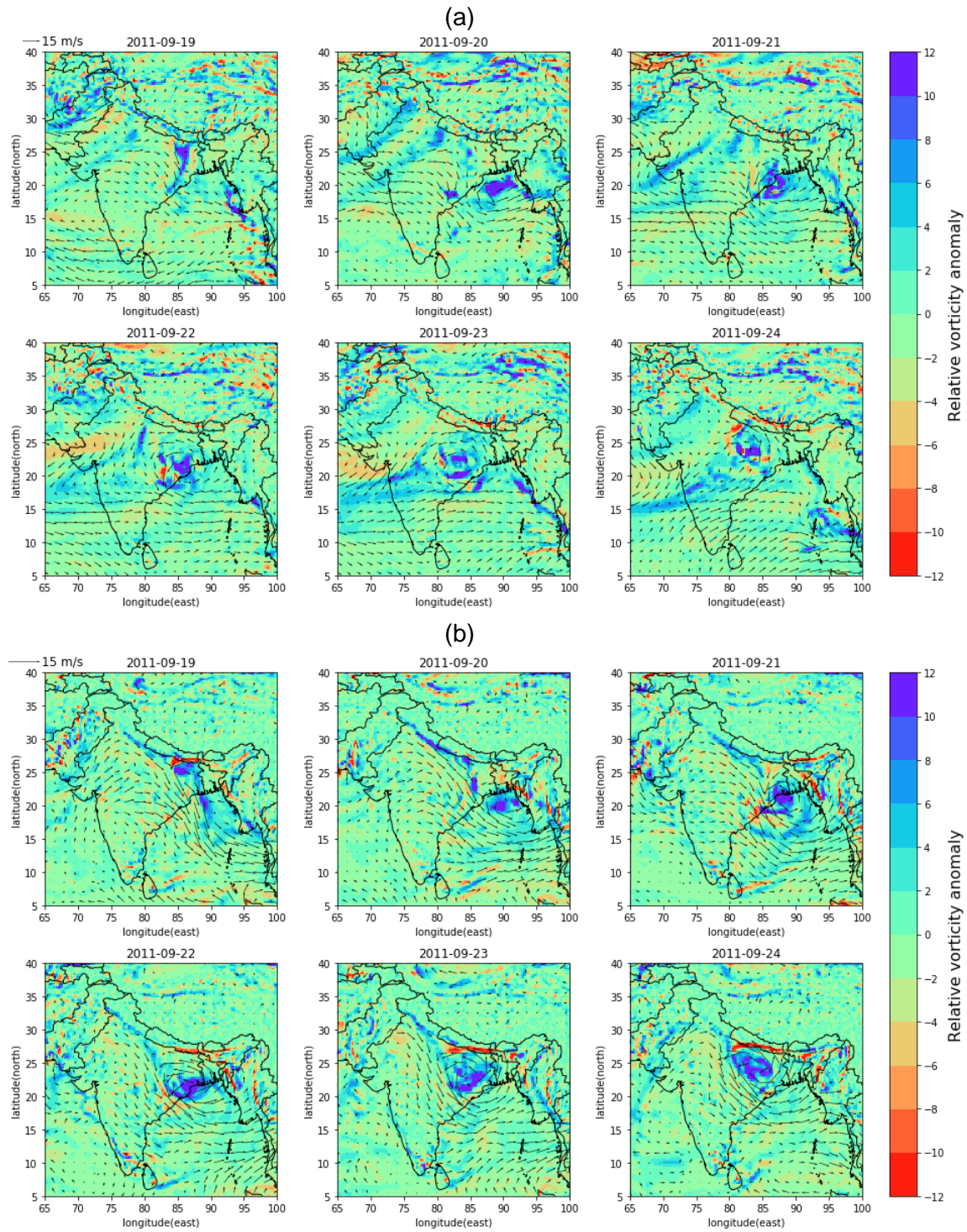


Figure 20. Horizontal pattern of relative vorticity anomaly (shaded) and wind velocity anomaly (vectors) from Day -3 to 2 (2011-09-22 - landfall day) for an MD during 2011 Sept 22-23 (an example from the BOTTOM list) at (a) 500 hPa, and (b) 850 hPa

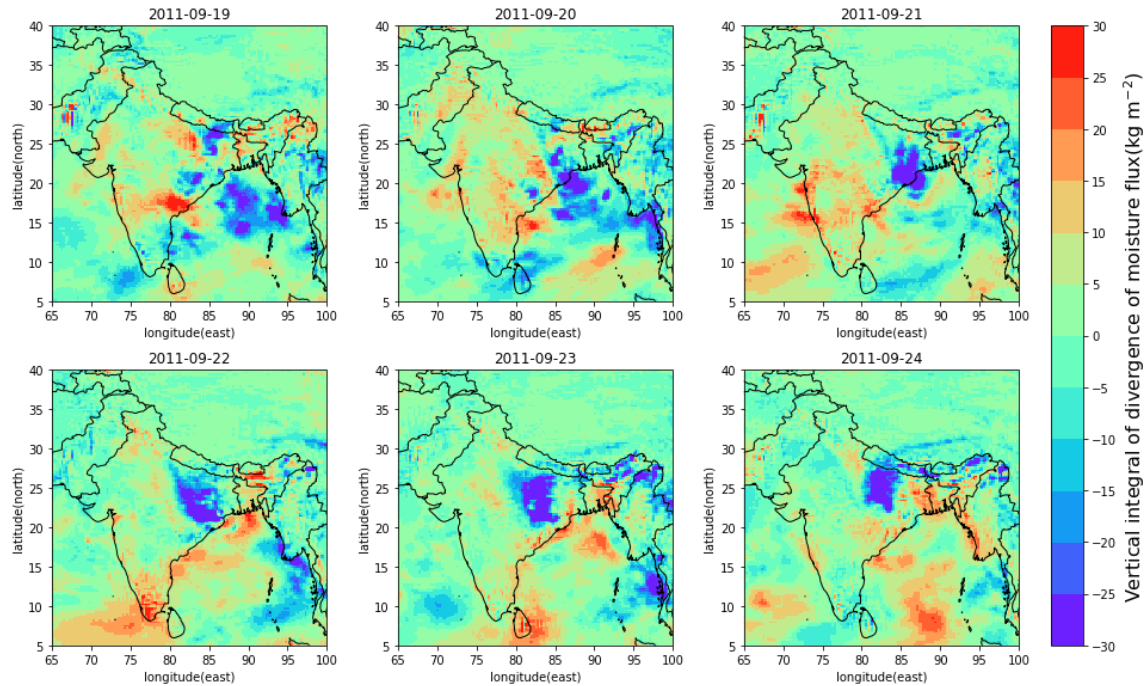


Figure 21. Horizontal pattern of VIDMF anomaly from Day -3 to 2 (2011-09-22 - landfall day) for an MD during 2011 Sept 22-23 (an example from the BOTTOM list)

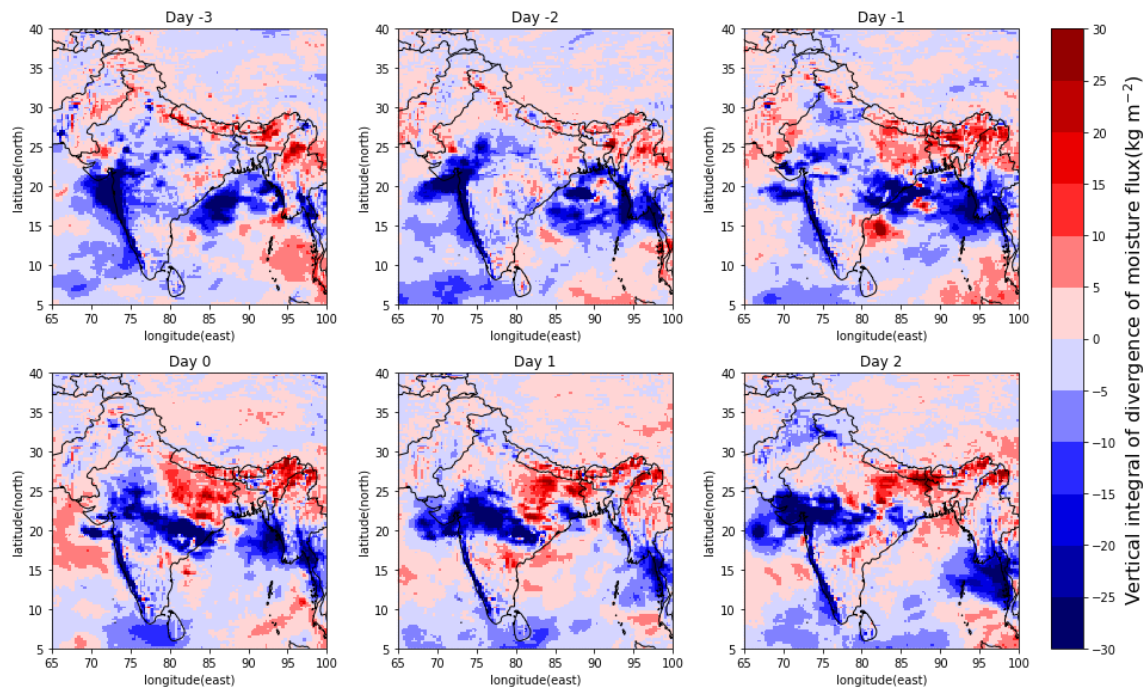


Figure 22. Difference between VIDMF ( $\text{kgm}^{-2}$ ) of composite TOP and composite BOTTOM

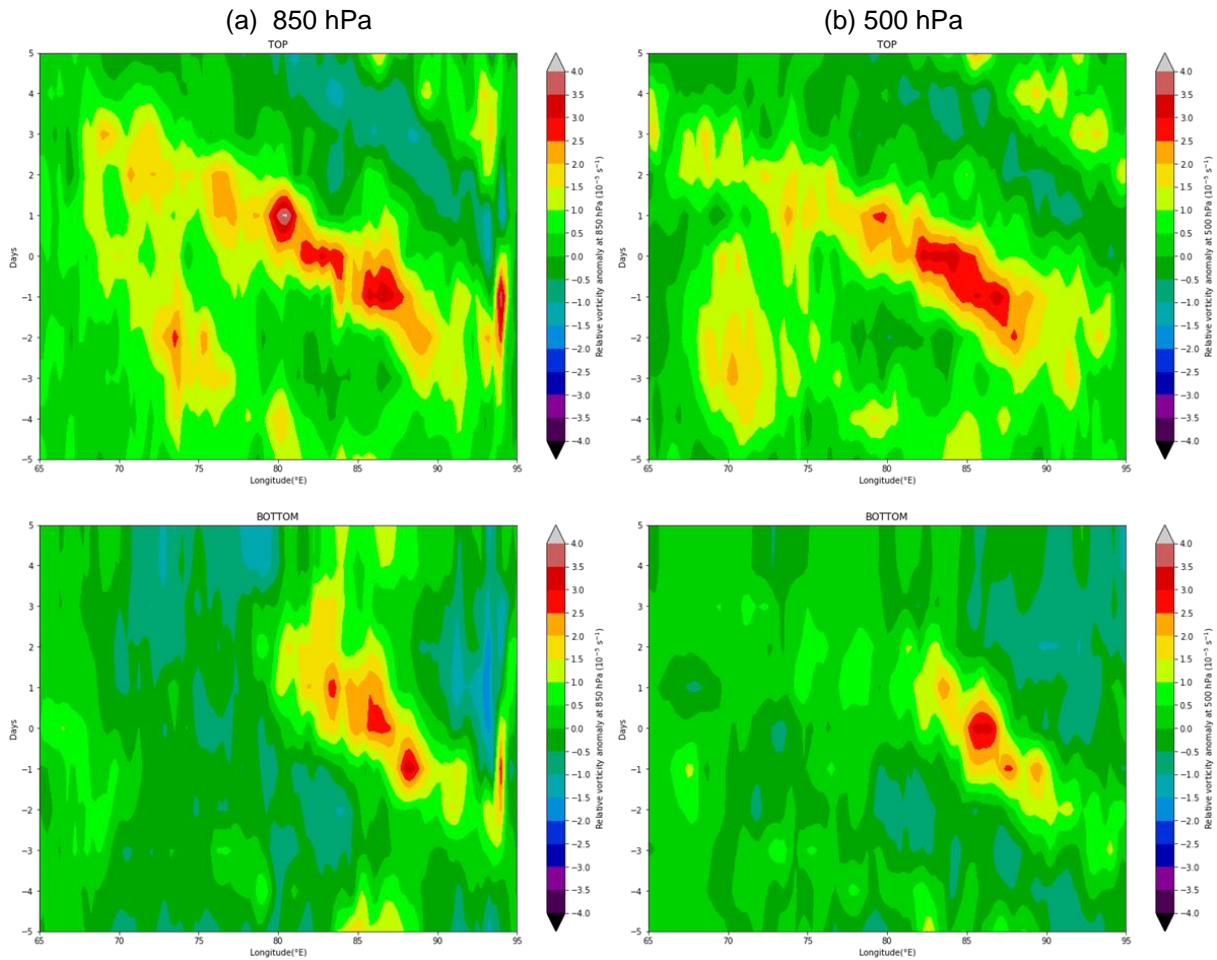


Figure 23. Hovmöller diagram of relative vorticity anomaly from Day -5 to Day 5, with longitude on the x-axis (a) at 850 hPa and (b) at 500 hPa. Values are latitudinally averaged between 15-26°N. Upper panel figures show TOP composites and lower panel figures show BOTTOM composites.

The VIDMF field (Figure 24) also shows the difference in the westward extent of moisture convergence flux. From both Figures 22 and 23, it appears like the westward propagation speed is slightly slower for MDs in the BOTTOM case. As mentioned previously, this is because the TOP case has a west-northwestward movement whereas the BOTTOM case has a north-westward movement. The remarkable difference between the two groups is that the TOP case features cyclonic vorticity on a longitudinal range corresponding to Gujarat state, even before the formation of MDs in the BoB and persists till the MD approach there, but the BOTTOM case does not. For the TOP case, large values of negative VIDMF (which indicates moisture convergence due to MTC) are present even from Day -5 onwards, as centered around 73°E, which peak on Day -3.

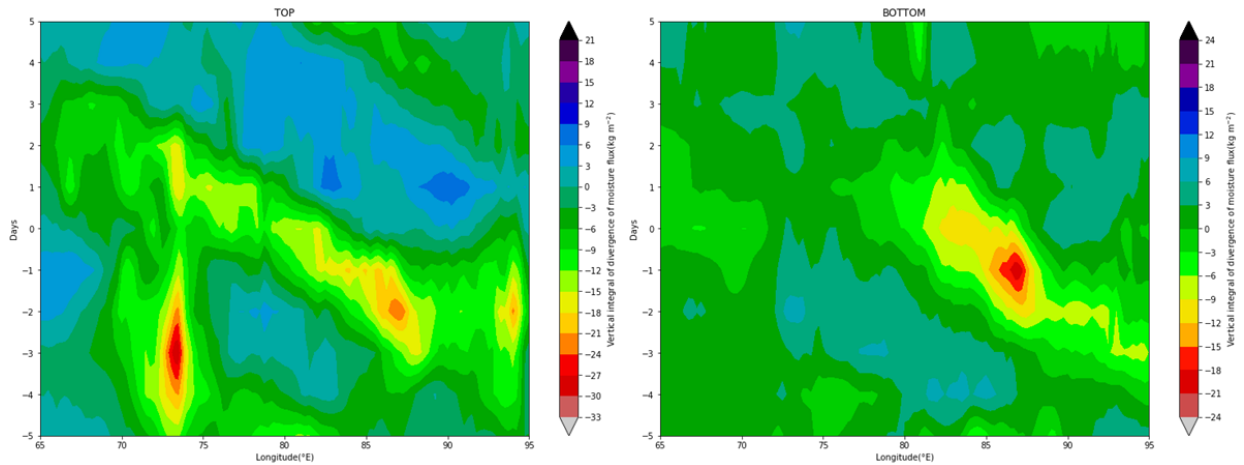


Figure 24. Hovmöller diagram of VIDMF from Day -5 to 5, with longitude on the x-axis (latitudinally averaged between 15-26°N). Left side- TOP composite, and right side- BOTTOM composite.

Whereas negative VIDMF associated with MDs appears and peaks at a later stage thus indicating the prior occurrence of MTC ahead of BoB MDs. For the BOTTOM case, 73° E is having the opposite sign for VIDMF (moisture divergence) thus ruling out the presence of MTC.

Note that current work has not addressed some other important questions thus requiring more detailed investigations which define the future outlook for this study. For example, what are the exact dynamical and thermodynamic processes through which MTC influences deeper penetration of MDs? Whether the increased soil moisture over central Indian plains can solely help to sustain MD activity or play only a secondary role in the land intrusion of MDs? Nevertheless, it is clear from the qualitative analysis that the cyclonic vorticity over the North-East Arabian Sea, Gujarat, and coastal Maharashtra brings moisture from the Arabian sea and increases the water vapor availability at least up to mid-troposphere above Northwest and central India. This establishes a background moisture and circulation environment that is conducive to MD intensification, and also through dynamical processes, it helps to maintain the MD to propagate across the Indian landmass. Further, the longitudinally stretched elliptical cyclonic circulation when MD approaches near Northwest India is also an indication of some important dynamical linkage thus causing an MTC-associated MD intruding into the Indian landmass, which needs to be investigated in detail as future work.

## 4. Summary and conclusions

The MDs are the predominant systems that are responsible for more than half of the ISMR with significant precipitation in and around their propagation paths. Subsequently, MDs have the potential to produce catastrophic flood conditions with tremendous effects, therefore their IPL and residence time over Indian landmass are important factors to consider. Despite the fact that the landfalling MDs often degrade quickly owing to the lower moisture flux and energy flux over land as compared to the ocean, occasionally they can persist longer and travel several hundred kilometers into the Indian landmass thus inflicting devastating flood conditions.

Some modeling studies inferred that the pre-storm soil moisture condition has a significant impact on MD duration and its inland penetration, which is hard to observationally verify as the long-term record of soil moisture observations are lacking over the Indian monsoon region. Recently, one observational study (Kishtawal et al. 2013) used antecedent rainfall data as a proxy for ground wetness to demonstrate the association of soil moisture (due to prestorm rainfall) on the persistence of MDs over land. However, this study gives importance only for the soil moisture originated locally and not remotely, thus requiring more investigations.

So, taking consideration of this limitation, firstly the current work utilized GLDAS reanalysis data for soil moisture in an effort to examine the significance of this surface parameter on the persistence of landfalling MDs, by a comprehensive examination of the long-lived and short-lived MDs. This is a first seminal attempt to qualitatively use the observed soil moisture data for establishing the association of inland penetration of MDs with the soil moisture. As soil moisture is a local surface parameter, we assume that any impact on MD is likely to be small-scale. So, for each MD, we only considered a square box with a dimension of  $5.5^\circ$ , with the MD's location in the center after two days of landfall. We go back three days prior to the day the MD is exactly over the chosen area and compare the soil moisture content (spatial distribution) for MDs with greater IPL (TOP cases) and MDs with shorter IPL (BOTTOM cases). By doing this, we are considering the diversity in MDs' track thus facilitating us to look at more regional influences.

Our results effectively show a positive soil moisture anomaly in a large portion of selected area for the TOP minus BOTTOM storm-centered composites in all the phases (from Day -1 to Day 2). This reveals that long-lived MDs had higher soil wetness over the area ahead of the MD compared to short-lived MDs. So, soil moisture can be considered one of the driving factors that aid in the maintenance of MD activity and allows it to penetrate deeper into the land before dissipation. In line with prior investigations, it thus comprehensively demonstrates a link between soil moisture and landfalling MD activity. However, this leaves us with some important questions for the future investigations. For example, are these findings statistically significant? How exactly the wet soil moisture creates a condition favorable for prolonging the lifetime of MD? Whether the enhanced soil moisture over central Indian plains can solely help to sustain MD activity or play only a secondary role in the land intrusion of MDs?

Another intriguing point is that it is still unclear whether any large-scale atmospheric circulation features can potentially influence the duration and dissipation of MDs which prompted us to further explore in this direction. Our subsequent analysis interestingly demonstrated that all long-lived MDs (TOP cases) have co-occurring (prior-landfall/post-landfall) MTCs with mid-tropospheric cyclonic vorticity over the northeastern Arabian sea near Gujarat, whereas it is conspicuously absent in the BOTTOM cases. To be precise, only 1 MD is accompanied by MTC in the BOTTOM group (out of 10 BOTTOM cases). This does not seem to be a coincidence, and we argue that there must be a dynamical linkage between Arabian sea MTC and BoB MD, and subsequently, the existence of the MTC might have played a significant role in facilitating the conditions favorable for the deeper intrusions of TOP MDs' into Indian landmass (i.e., longer IPL).

Northwest India is found to be having increased convergence of vertically integrated moisture flux for MDs of TOP case. This is due to the cyclonic vorticity associated with MTC which transports moist Arabia Sea air to the Indian subcontinent. The same region acts as a diverging center of moisture flux for BOTTOM cases, due to the anticyclonic circulation patterns which may cause dry air intrusion from heat low over Rajasthan and Pakistan region, thus creating background moisture conditions unfavorable for the sustenance of MD structure which results in the rapid dissipation of MD thus limiting

its progression into the Indian landmass. In contrast, for the TOP cases, MTC acts as a source of moisture content for the atmospheric column over northwest India, and an MD reaching the central India might be exposed to abundant water vapor content to sustain the MD over landmass and thus allowing them to intrude further westward. Further, the longitudinally stretched cyclonic circulation when MD approaches near Northwest India is also an indication of some important dynamical linkage, which needs to be investigated in detail as future work.

While the systems in the TOP group moved in a west-northwest direction toward the MTC, the systems in the BOTTOM group generally followed a northwest direction. This raises some intriguing questions: does MTC play a role in altering the path of MD propagation? If yes, what might be the plausible dynamics by which it modifies the propagation mechanism proposed by earlier studies? This defines the future prospects of this study.

In brief, our results provide the first seminal evidence that the presence of MTC over northeastern Arabian sea, which in conjunction with wet soil conditions, create favorable conditions for a prolonged duration of BoB MD over Indian subcontinent. Thus, it suggests a possibility that intense MDs with a potential to travel more distance over the Indian landmass in a west-northwestward direction can be predicted (i.e., short-term prediction) by systematically monitoring these antecedent MTCs (and its associated circulation) as formed over the Gujarat region. Our study assumes further importance, as a recent study showed increasing trend in the extreme daily rainfall intensities over northwest to central Indian plains (You and Ting 2021) which calls for careful monitoring of MTCs and BoB MDs so as to better anticipate the flood producing daily rainfall extremes thus enabling us to lessen their disastrous impacts.

# References

1. AjayaMohan R. S., Merryfield W. J., Kharin V. V. (2010). Increasing trend of synoptic activity and its relationship with extreme rain events over central India, *Journal of Climate*, 23, 1004–1013
2. Baisya, H., Pattnaik, S., & Rajesh, P. V. (2017). Land surface-precipitation feedback analysis for a landfalling monsoon depression in the Indian region. *Journal of Advances in Modeling Earth Systems*, 9(1), 712-726.
3. Boos, W., Hurley, J. and Murthy, V. (2015) Adiabatic westward drift of Indian monsoon depressions. *Quarterly Journal of the Royal Meteorological Society*, 141, 1035– 1048.
4. Carr, F. H. (1977). Mid-tropospheric cyclones of the summer monsoon. *Pure and applied geophysics*, 115, 1383-1412.
5. Charney, J. G. and Eliassen, A. (1964) On the growth of the hurricane depression, *Journal of Atmospheric Sciences*, 21, 68–7
6. Cohen, N. Y., and W. R. Boos. (2014) Has the number of Indian summer monsoon depressions decreased over the last 30 years? *Geophysical Research Letters*, 41, 7846–7853
7. Cohen, N. Y. and Boos, W. R. (2016) Perspectives on moist baroclinic instability: implications for the growth of monsoon depressions, *Journal of the Atmospheric Sciences*, 73, 1767–1788.
8. Chang, H. I., Niyogi, D., Kumar, A., Kishtawal, C. M., Dudhia, J., Chen, F., ... & Shepherd, M. (2009) Possible relation between land surface feedback and the post-landfall structure of monsoon depressions. *Geophysical Research Letters*, 36(15).
9. Choudhury, A. D., Krishnan, R., Ramarao, M. V. S., Vellore, R., Singh, M., & Mapes, B. (2018). A phenomenological paradigm for midtropospheric cyclogenesis in the Indian summer monsoon. *Journal of the atmospheric sciences*, 75(9), 2931-2954.
10. Dastoor, A., & Krishnamurti, T. N. (1991). The landfall and structure of a tropical cyclone: The sensitivity of model predictions to soil moisture parameterizations. *Boundary-layer meteorology*, 55(4), 345-380.
11. Davis CA. 1992. Piecewise potential vorticity inversion. *Journal of Atmospheric Science*, 49, 1397– 1411.
12. Francis, P. A., & Gadgil, S. (2006). Intense rainfall events over the west coast of India. *Meteorology and Atmospheric Physics*, 94(1-4), 27-42



13. Gadgil, S. (2018) The monsoon system: Land–sea breeze or the ITCZ?, *Journal of Earth System Science*, 127, 1
14. Gill, A. E. (1980) Some simple solutions for heat-induced tropical circulation, *Quarterly Journal of the Royal Meteorological Society*, 106, 447-462
15. Godbole, R. V. (1977) The composite structure of the monsoon depression, *Tellus* 29,25–40
16. Goswami, B. A. (1987) A mechanism for the west-north-west movement of monsoon depressions. *Nature* 326, 376–378
17. Hersbach, H., Bell, B., Berrisford, P., Hirahara, S., Horányi, A., Muñoz-Sabater, J., ... & Thépaut, J. N. (2020). The ERA5 global reanalysis. *Quarterly Journal of the Royal Meteorological Society*, 146(730), 1999-2049
18. Hunt, K., Turner, A. G., Inness, P. M., Parker, D. E., Levine, R. C. (2016a) On the structure and dynamics of Indian monsoon depressions. *Monthly Weather Review*, 144, 3391–3416.
19. Hunt, K. M. R., Turner, A. G. and Parker, D. E. (2016b) The spatiotemporal structure of precipitation in Indian monsoon depressions. *Quarterly Journal of the Royal Meteorological Society*, 142(701), 3195– 3210.
20. Hunt, K. M., & Turner, A. G. (2017). The effect of soil moisture perturbations on Indian monsoon depressions in a numerical weather prediction model. *Journal of Climate*, 30(21), 8811-8823.
21. Joseph, P. V. and Chakravorthy, K. K., 1980, "Lower tropospheric temperature structure of the monsoon depression", 11-14 August 1979', Results of Summer MONEX field phase research (Part B), FGGE Operations Report, 9, 257-265.
22. Kaplan, J., and DeMaria, M. (1995) A simple empirical model for predicting the decay of tropical cyclone winds after landfall, *Journal of Applied Meteorology and Climatology*. 34 (11), 2499–2512.
23. Kellner, O., Niyogi, D., Lei, M., and Kumar, A. (2012) The role of anomalous soil moisture on the inland reintensification of Tropical Storm Erin (2007). *Nat. Hazards*, 63, 1573-1600
24. Kishtawal, C. M., Niyogi, D., Rajagopalan, B., Rajeevan, M., Jaiswal, N., & Mohanty, U. C. (2013). Enhancement of inland penetration of monsoon depressions in the Bay of Bengal due to prestorm ground wetness. *Water resources research*, 49(6), 3589-3600
25. Krishnamurthy, V. and AjayaMohan, R.S. (2010) Composite structure of monsoon low-pressure systems and its relation to Indian rainfall. *Journal of Climate*, 23, 4285–4305

26. Krishnamurti, T. N., & Hawkins, R. S. (1970). Mid-tropospheric cyclones of the southwest monsoon. *Journal of Applied Meteorology and Climatology*, 9(3), 442-458.
27. Krishnamurthy, V., and Shukla, J. (2007) Intraseasonal and seasonally persisting patterns of Indian monsoon rainfall. *Journal of Climate*, 20, 3–20
28. Krishnamurti, T. N., Kanamitsu, M., Godbole, R., Chang, C-B., Carr, F., and. Chow, J. H. (1975) Study of a monsoon depression (I): Synoptic structure, *Journal of the Meteorological Society of Japan*, **53**, 227–239
29. Kumar, A., Dudhia, J., Rotunno, R., Niyogi, D., & Mohanty, U. C. (2008). Analysis of the 26 July 2005 heavy rain event over Mumbai, India using the Weather Research and Forecasting (WRF) model. *Quarterly Journal of the Royal Meteorological Society*, 134(636), 1897-1910
30. Kushwaha, P., Sukhatme, J., & Nanjundiah, R. (2021). A Global Tropical Survey of Midtropospheric Cyclones, *Monthly Weather Review*, 149(8), 2737-2753.
31. Kushwaha, P., Sukhatme, J., & Nanjundiah, R. S. (2022). Classification of Middle Tropospheric Systems over the Arabian Sea and Western India
32. Mak, M. K. (1975). The monsoonal mid-tropospheric cyclogenesis. *Journal of Atmospheric Sciences*, 32(12), 2246-2253.
33. Miller, F. R. and Keshavamurthy, R. N. (1968), Structure of an Arabian Sea summer monsoon system, *Meteorological Monograph 1*, East-West Center Press, 94
34. Meera, M., Suhas, E., Sandeep, S. (2019) Downstream and in Situ: two Perspectives on the Initiation of Monsoon Low-pressure Systems over the Bay of Bengal, *Geophysical Research Letters*, 46, 12303-12310
35. Mooley, D. A. (1973) Some Aspects of Indian Monsoon Depressions and the Associated Rainfall, *Monthly Weather Review*, 101, 271-280
36. Mooley, D. A., Shukla, J. (1987) Characteristics of the westward-moving summer monsoon low pressure systems over the Indian region and their relationship with the monsoon rainfall, *University of Maryland Center for Ocean-Land-Atmosphere Interactions Rep.*, 47
37. Mulky, G. R., Banerji, A. K. (1960) The mean upper wind circulation around monsoon depressions in India, *Journal of Meteorology*, 17, 8–14.
38. Pai, D. S., Rajeevan, M., Sreejith, O. P., Mukhopadhyay, B., & Satbha, N. S. (2014). Development of a new high spatial resolution (0.25× 0.25) long period (1901-2010) daily gridded rainfall data set over India and its comparison with existing data sets over the region. *Mausam*, 65(1), 1-18

39. Ramage, C. S. (1966). The summer atmospheric circulation over the Arabian Sea. *Journal of Atmospheric Sciences*, 23(2), 144-150
40. Rao, Y. P. (1976) "Southwest Monsoon", *Meteorological Monograph, Synoptic Meteorology*, 1/76, India Meteorological Department, 140.
41. Ray, K., Pandey, P., Pandey, C., Dimri, A. P., & Kishore, K. (2019). On the recent floods in India. *Current science*, 117(2), 204-218
42. Rodell, M., Houser, P. R., Jambor, U. E. A., Gottschalck, J., Mitchell, K., Meng, C. J., ... & Toll, D. (2004). The global land data assimilation system. *Bulletin of the American Meteorological society*, 85(3),381-394
43. Saha, K. and Saha, S. (1988) Thermal budget of a monsoon depression in the Bay of Bengal during FGGE-MONEX 1979, *Monthly Weather Review*, 116,242–254
44. Saha, K., Sanders, F., Shukla, J. (1981) Westward propagating predecessors of monsoon depressions, *Monthly Weather Review*, 109,330–343
45. Shyamala, B., & Bhadram, C. V. V. (2006). Impact of mesoscale–synoptic scale interactions on the Mumbai historical rain event during 26–27 July 2005. *Current Science*, 1649-1654
46. Sikka, D. R. (1977) Some aspects of the life history, structure and movement of monsoon depressions, *Pure and Applied Geophysics*, 115, 1501–1529
47. Sikka, D. R. (2006) A study on the monsoon low pressure systems over the Indian region and their relationship with drought and excess monsoon seasonal rainfall, *Center for Ocean-Land-Atmosphere Studies Technical Report*, 217, 61
48. Webster, P.J., Clark, C., Cherikova, G., Fasullo, J., Han, W., Loschnigg, J., Kamran Sahami. (2002) *The monsoon as a self-regulating coupled ocean-atmosphere system*, Editor: R.P. Pearce, *International Geophysics*, 83, 198-219
49. Yoon, J.-H., Chen, T. C. (2005) Water vapor Budget of the Indian monsoon depression, *Tellus*, 57A, 770–782
50. You Y and Ting M (2021) Observed trends in the South Asian monsoon low-pressure systems and rainfall extremes since the late 1970s. *Geophysical Research Letters*, 48

